# Classical, Nonclassical, and Mixed-Metal Osmium(II) Polyhydrides Stabilized by the Tetraphosphine $P(CH_2CH_2PPh_2)_3$. H/D Isotope Exchange Reactions Promoted by a Strongly Bound Dihydrogen Ligand

**Claudio Bianchini,* Klaus Linn, Dante Masi, Maurizio Peruzzini, Alfonso Polo,† Alberto Vacca, and Fabrizio Zanobini**

Istituto per lo Studio della Stereochimica ed Energetica dei Composti di Coordinazione, CNR, Via J. Nardi 39, 50132 Firenze, Italy

*Received September 22, 1992*

The *cis*-hydride-$\eta^2$-dihydrogen complex $[(PP_3)OsH(\eta^2\text{-}H_2)]BPh_4$ (**4**), $PP_3 = P(CH_2CH_2PPh_2)_3$, has been prepared by either protonation of the dihydride $[(PP_3)OsH_2]$ or reaction of the novel dinitrogen complex $[(PP_3)OsH(N_2)]BPh_4$ (**6**) with $H_2$. The nonclassical structure of **4** has been established in solution by variable-temperature NMR spectroscopy ($^1H$, $^{31}P$), $T_1$ measurements, and $J(HD)$ values. An X-ray diffraction analysis has shown that the solid-state geometry of the compound is not inconsistent with the nonclassical assignment. Crystals of **4** are triclinic, space group $P\bar{1}$ with $a = 16.841(4)$ Å, $b = 15.135(2)$ Å, $c = 12.450(3)$ Å, $\alpha = 91.53(2)°$, $\beta = 96.07(2)°$, $\gamma = 106.75(2)°$, $V = 3016.23$ Å$^3$, and $Z = 2$. In the solid state and in solution at low temperature, $[(PP_3)OsH(\eta^2\text{-}H_2)]^+$ is octahedral and the hydride and dihydrogen ligands occupy mutually cis positions. The $H_2$ ligand is trans to the bridgehead phosphorus of $PP_3$. At ambient temperature, **4** is highly fluxional. The dynamic behavior of the complex in solution has been studied by variable-temperature $^{31}P\{^1H\}$ NMR spectroscopy using the DNMR3 program. A comparison of the chemical properties, in particular $H_2$-displacement reactions, within the series $[(PP_3)MH(\eta^2\text{-}H_2)]^+$ (M = Fe, Ru, Os) leads to the conclusion that the osmium complex has the strongest interaction with the $H_2$ ligand. Complex **4** has been found capable of reacting with $(CD_3)_2CO$ to give the perdeuterated isotopomer **4**-$d_3$ via a keto-enol tautomerization reaction of acetone-$d_6$. The isolation and characterization of the mixed osmium-gold dihydride $[(PP_3)OsH\{\eta^2\text{-}HAu(PPh_3)\}]PF_6$ has provided experimental evidence for the correctness of the $H_2$ and $HAu(PPh_3)$ isolobal relationship. The dinitrogen ligand in **6** can easily be displaced by a plethora of ligands, including weak ones such as THF and acetone. The latter reagent reacts with **6** to form the first example of a stable and isolable *cis*-hydride-$\eta^1$-ketone complex, $[(PP_3)OsH\{\eta^1\text{-}OC(CH_3)_2\}]BPh_4$, a suggested key intermediate in metal-assisted hydrogenation reactions of ketones.

## Introduction

The potentially tetradentate ligand $P(CH_2CH_2PPh_2)_3$ ($PP_3$) is able to form stable Fe(II) and Ru(II) *cis*-hydride-$\eta^2$-dihydrogen complexes of the formula $[(PP_3)MH(\eta^2\text{-}H_2)]BPh_4$ (I).[1,2] Re-

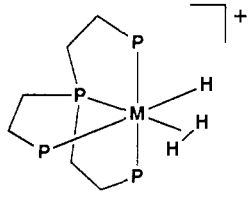


I

M = Fe, Ru

activity studies have clearly shown that the solution chemistry of these nonclassical trihydrides is dominated by the different metal-dihydrogen bond strength, which phenomenologically increases in the order Ru < Fe.[1,3-6] Direct experimental evidence of a larger $d\pi(M)\text{-}\sigma^*(H_2)$ back-donation for iron has been obtained by inelastic neutron scattering experiments, which give a higher barrier to rotation of the dihydrogen ligand in the iron derivative.[7]

We, therefore, decided to synthesize the osmium(II) analogue, $[(PP_3)OsH(\eta^2\text{-}H_2)]BPh_4$, with the aim to compare its spectroscopic and chemical properties with those of the Fe and Ru congeners. This type of investigation has recently been carried out by Morris and co-workers on the series of complexes $[MH(\eta^2\text{-}H_2)(L)_2]^+$, where M = Fe, Ru, and Os and L = $Et_2PCH_2CH_2PEt_2$ (depe) or $Ph_2PCH_2CH_2PPh_2$ (dppe).[8] A multiform experimental study led these investigators to the conclusion that the metal-dihydrogen bond strength increases in the order Ru < Fe < Os, while the H-H interactions decrease correspondingly.

In case of the $PP_3$ complexes, the question of the M-$H_2$ bond strength is not merely academic. In fact, the Fe and Ru compounds have been found to efficiently catalyze a variety of homogeneous reactions with mechanisms and selectivities that depend on the nature of the metal to dihydrogen bond.[1,3-6] Since preliminary tests show $[(PP_3)OsH(\eta^2\text{-}H_2)]BPh_4$ to have potential in homogeneous catalysis, a deep knowledge of the spectroscopic and chemical properties is expected to bring about a more convenient and appropriate use of the Os complex as a reagent, particularly in terms of types of reactions and proper experimental conditions.

† Present address: Departament de Química, Facultat de Ciències Experimentals i de la Salut, Universitat de Girona, Pl. Hospital 6, 17071 Girona, Spain.

(1) Bianchini, C.; Peruzzini, M.; Polo, A.; Vacca, A.; Zanobini, F. *Gazz. Chim. Ital.* **1991**, *121*, 543.
(2) Bianchini, C.; Perez, P. J.; Peruzzini, M.; Zanobini, F.; Vacca, A. *Inorg. Chem.* **1991**, *30*, 279.
(3) Bianchini, C.; Meli, A.; Peruzzini, M.; Frediani, P.; Bohanna, C.; Esteruelas, M. A.; Oro, L. A. *Organometallics* **1992**, *11*, 138.
(4) Bianchini, C.; Peruzzini, M.; Zanobini, F.; Frediani, P.; Albinati, A. *J. Am. Chem. Soc.* **1991**, *113*, 5453.
(5) Bianchini, C.; Farnetti, E.; Frediani, P.; Graziani, M.; Peruzzini, M.; Polo, A. *J. Chem. Soc., Chem. Commun.* **1991**, 1336.
(6) Bianchini, C.; Bohanna, C.; Esteruelas, M. A.; Frediani, P.; Meli, A.; Oro, L. A.; Peruzzini, M. *Organometallics* **1992**, *11*, 3837.
(7) Eckert, J.; Albinati, A.; White, R. P.; Bianchini, C.; Peruzzini, M. *Inorg. Chem.* **1992**, *31*, 4241.
(8) Bautista, M. T.; Cappellani, E. P.; Drouin, S. D.; Morris, R. H.; Schweitzer, C. T.; Sella, A.; Zubkowski, J. *J. Am. Chem. Soc.* **1991**, *113*, 4876 and references therein.

0020-1669/93/1332-2366$04.00/0 

**Scheme I**

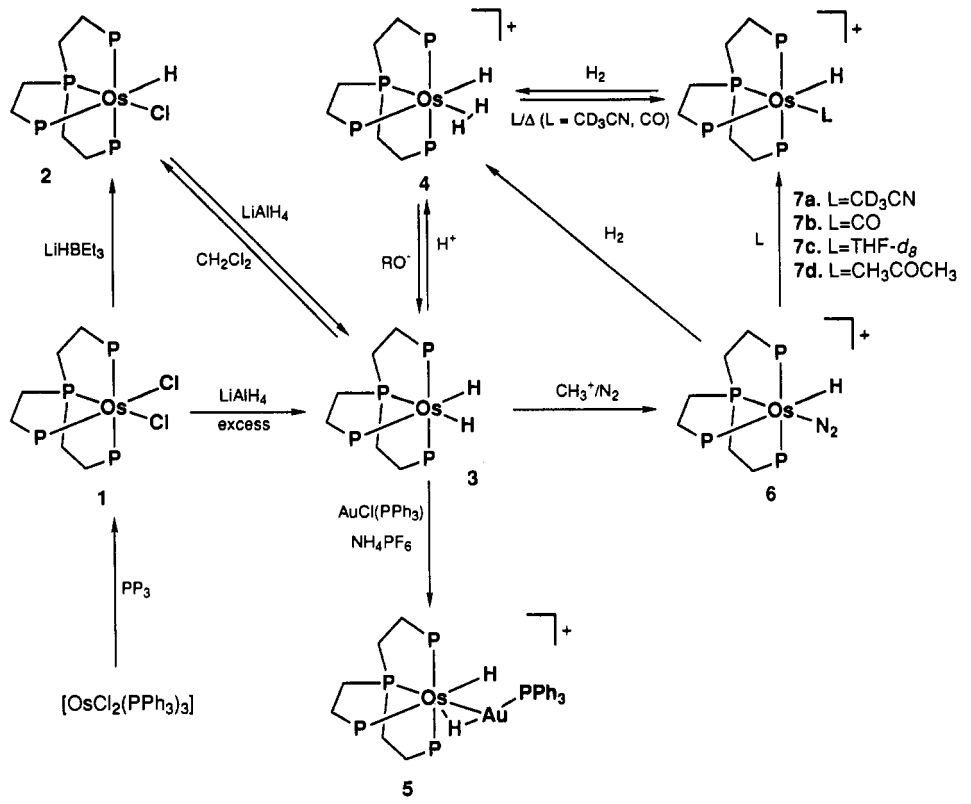


In this paper, we describe the synthesis and characterization of $[(PP_3)OsH(\eta^2\text{-}H_2)]BPh_4$ and of a related family of mono- and dihydrido complexes, including a mixed Os–Au dihydride which provides further, convincing experimental evidence of the isolobal relationship between the "H" and "Au($PPh_3$)" moieties.[9] Of particular relevance is also the complex $[(PP_3)OsH(N_2)]BPh_4$ from which the $N_2$ ligand can easily be displaced by a variety of weak-donor molecules, including acetone. As a result, a rare example of a *cis*-hydride–$\eta^1$-*O*-OCRR′ complex, $[(PP_3)OsH\{\eta^1\text{-}O\text{-}OC(CH_3)_2\}]BPh_4$, has been isolated. Compounds of the latter type are of remarkable importance due to their participation as intermediate species in metal-assisted hydrogenation reactions of ketones and aldehydes.[10]

Finally, we report on an H/D isotope exchange reaction that converts $[(PP_3)OsH(\eta^2\text{-}H_2)]BPh_4$ to its perdeuterated isotopomer $[(PP_3)OsD(\eta^2\text{-}D_2)]BPh_4$ simply by dissolution in $CD_3COCD_3$.

## Results

**Synthesis and Characterization of the Complexes.** The preparations and principal reactions of the new complexes described in this paper are illustrated in Scheme I. Selected NMR spectral data are collected in Table I ($^{31}P\{^1H\}$ NMR spectra) and Table II ($^1H$ NMR spectra). The latter includes also IR absorbances assigned to $\nu$(Os–H) vibrational modes.

**$[(PP_3)OsCl_2]$.** The dichloride $[(PP_3)OsCl_2]$ (**1**) constitutes an excellent entry to osmium(II) hydride complexes stabilized by the tripodal tetradentate ligand $PP_3$. Compound **1** is synthesized in rather good yield (75%) by reaction of $[OsCl_2(PPh_3)_3]$ with an equivalent amount of $PP_3$ in refluxing 2-methoxyethanol for 3 h.

Compound **1** is a cream-colored crystalline material that can be purified by recrystallization from $CH_2Cl_2$/EtOH. The $^{31}P\{^1H\}$ NMR spectrum in $CD_2Cl_2$ consists of a temperature-invariant first-order $AMQ_2$ splitting pattern, which is typical for all octahedral (OCT) osmium complexes herein described.

The spectrum shows three well-separated resonances of relative intensities 1:1:2 ($AMQ_2$ splitting pattern). The highest frequency resonance at 114.68 ppm can unambiguously be attributed to the bridgehead phosphorus atom $P_A$ of the $PP_3$ ligand.[1,2,11,12] This resonance appears as a triplet of doublets and is originated by coupling to the two equivalent terminal phosphorus $P_Q$ trans to each other in the axial positions of the octahedron and to the remaining phosphorus atom $P_M$ trans to one of the two chloride ligands. The resonance of the terminal $P_M$ atom at 19.09 ppm consists of a triplet of doublets arising from coupling to the two equivalent terminal phosphorus, $P_Q$, and to the apical phosphorus, $P_A$. Finally, the remaining resonance, which appears as a doublet of doublets at 10.69 ppm, is ascribable to the two mutually trans phosphorus atoms $P_Q$. This multiplicity arises from coupling to the residual terminal phosphorus atom $P_M$ and to the bridgehead donor atom $P_A$.

(9) (a) Hoffmann, R. *Angew. Chem., Int. Ed. Engl.* **1982**, *21*, 711. (b) Stone, F. G. A. *Angew. Chem., Int. Ed. Engl.* **1984**, *23*, 89. (c) Lauher, J. W.; Wald, K. *J. Am. Chem. Soc.* **1981**, *103*, 7648. (d) Housecroft, C. E.; Rheingold, A. L. *Organometallics* **1987**, *6*, 1332. (e) Bateman, L. W.; Green, M.; Mead, K. A.; Mills, R. M.; Salter, I. D.; Stone, F. G.; Woodward, P. *J. Chem. Soc., Dalton Trans.* **1983**, 2599. (f) Bianchini, C.; Peruzzini, M.; Zanobini, F. *J. Organomet. Chem.* **1990**, *390*, C16. (g) Bruce, M. I.; Corbin, P. E.; Humphrey, P. A.; Koutsantonis, G. A.; Liddell, M. J.; Tiekink, E. R. T. *J. Chem. Soc., Chem. Commun.* **1990**, 674. (h) Salter, I. *Adv. Organomet. Chem.* **1989**, *29*, 260. (i) Hall, K. P.; Mingos, D. M. P. *Prog. Inorg. Chem.* **1984**, *32*, 237. (j) Bianchini, C.; Meli, A.; Peruzzini, M.; Vacca, A.; Vizza, F.; Albinati, A. *Inorg. Chem.* **1992**, *31*, 3841.

(10) (a) P. A. Challoner *Handbook of Coordination Catalysis in Organic Chemistry*; Butterwords & Co. Publishers: London, 1986; p 96. (b) Esteruelas, M. A.; Lahoz, F. J.; Lopez, J. A.; Oro, L. A.; Schlünken, C.; Valero, C.; Werner, H. *Organometallics* **1992**, *11*, 2034.

(11) (a) Bianchini, C.; Innocenti, P.; Meli, A.; Peruzzini, M.; Zanobini, F.; Zanello, P. *Organometallics* **1990**, *9*, 2514. (b) Bianchini, C.; Meli, A.; Peruzzini, M.; Vizza, F.; Frediani, P. *Organometallics* **1990**, *9*, 1146. (c) Bianchini, C.; Meli, A.; Peruzzini, M.; Zanobini, F.; Bruneau, C.; Dixneuf, P. *Organometallics* **1990**, *9*, 1155. (d) Bianchini, C.; Mealli, C.; Meli, A.; Peruzzini, M.; Zanobini, F. *J. Am. Chem. Soc.* **1988**, *110*, 8725. (e) Bianchini, C.; Meli, A.; Peruzzini, M.; Vizza, F.; Zanobini, F.; Frediani, P. *Organometallics* **1989**, *8*, 2080.

(12) (a) Bianchini, C.; Meli, A.; Peruzzini, M.; Ramirez, J. A.; Vacca, A.; Vizza, F.; Zanobini, F. *Organometallics* **1989**, *8*, 337. (b) Bianchini, C.; Masi, D.; Meli, A.; Peruzzini, M.; Ramirez, J. A.; Vacca, A.; Zanobini, F. *Organometallics* **1989**, *8*, 2179. (c) Gambaro, J. J.; Hohman, W. H.; Meek, D. W. *Inorg. Chem.* **1989**, *28*, 4154.

**Table I.** $^{31}P\{^1H\}$ NMR Data for the Complexes

| comp | solvent | temp, K | pattern | chem shift, ppm[a] | | | coupling const J, Hz | | |
|---|---|---|---|---|---|---|---|---|---|
| | | | | $\delta(P_A)$ | $\delta(P_M)$ | $\delta(P_Q)$ | $P_AP_M$ | $P_AP_Q$ | $P_MP_Q$ |
| **1** | $CD_2Cl_2$ | 296 | $AMQ_2$ | 114.68 | 19.09 | 10.69 | 7.3 | 8.9 | 11.4 |
| **2** | $CD_2Cl_2$ | 296 | $AMQ_2$ | 113.16 | 16.27 | 17.81 | 8.1 | 3.5 | 7.6 |
| **3** | $C_6D_6$ | 333 | $AM_3$ | 134.91 | 45.35 | | 4.8 | | |
| | $CD_2Cl_2$ | 296 | $AM_3$ | 133.69 | 44.07 | | 4.1 | | |
| | | 198 | $AMQ_2$ | 132.19 | 46.46 | 43.22 | 11.2 | *b* | 6.4 |
| **4** | $CD_2Cl_2/CFCl_3$ | 296 | $AM_3$ | 119.36 | 34.29 | | 2.1 | | |
| | | 153 | $AMQ_2$ | 117.45 | 47.10 | 28.10 | *b* | *b* | *b* |
| | $CD_2Cl_2$ | 296 | $AM_3$ | 120.41 | 34.34 | | 2.0 | | |
| **4-$d_1$** | $CD_2Cl_2$ | 296 | $AM_3$ | 120.24 | *d* | | *b* | | |
| **4-$d_2$** | $CD_2Cl_2$ | 296 | $AM_3$ | 120.09 | *d* | | *b* | | |
| **4-$d_3$** | $CD_2Cl_2$ | 296 | $AM_3$ | 119.95 | *d* | | *b* | | |
| **5**[c] | $CD_2Cl_2$ | 296 | $AM_3X$ | 126.35 | 32.60 | | 3.2 | | |
| | | 233 | $AMQ_2X$ | 125.60 | 49.34 | 30.58 | 4.6 | *b* | 8.7 |
| **6** | $CD_2Cl_2$ | 296 | $AMQ_2$ | 109.00 | 23.80 | 24.21 | 3.6 | 2.3 | 5.3 |
| **7a** | $CD_3CN$ | 296 | $AMQ_2$ | 113.80 | 24.46 | 24.00 | 7.1 | 3.7 | 6.6 |
| **7b** | $CD_2Cl_2$ | 296 | $AMQ_2$ | 115.29 | 30.78 | 27.33 | 5.6 | 3.5 | 5.7 |
| **7c** | TDF | 296 | $AMQ_2$ | 102.60 | 33.54 | 31.11 | 13.3 | 7.0 | 5.0 |
| **7d** | $CD_2Cl_2$ | 296 | $AMQ_2$ | 106.10 | 25.40 | 31.45 | 13.1 | 5.5 | 6.5 |

[a] Chemical shift values ($\delta$'s) are relative to 85% $H_3PO_4$ with positive values being downfield from the standard. $P_A$ refers to the bridgehead phosphorus atom of the $PP_3$ ligand, whereas $P_M$ and $P_Q$ denote the terminal phosphorus atoms. [b] Broad resonances. [c] $P_X$ refers to the triphenylphosphine ligand. At 296 K $\delta(P_X)$ = 55.08 ppm, $J(P_AP_X)$ = 29.5 Hz, $J(P_MP_X)$ = 3.5 Hz; at 233 K $\delta(P_X)$ = 54.20, $J(P_AP_X)$ = 28.9 Hz, $J(P_MP_X)$ = 18.1 Hz, $J(P_QP_X)$ = 3.7 Hz. [d] Broad resonance at ca. 34.3 ppm.

The splitting pattern, chemical shifts, and coupling constants observed for $[(PP_3)OsCl_2]$ (Table I) are therefore consistent with an OCT geometry around osmium(II) in which the two chloride ligands are forced cis by the geometrical requirements of the tripodal ligand.

**$[(PP_3)OsHCl]$.** When **1** in THF solution is reacted with a stoichiometric amount of $LiHBEt_3$ (1.0 M in THF), a fast reaction takes place to give pale yellow crystals of the *cis*-hydride–chloride complex $[(PP_3)OsHCl]$ (**2**).

Complex **2** exhibits a temperature-invariant first-order $^{31}P\{^1H\}$ NMR $AMQ_2$ spin system ($CD_2Cl_2$), pointing to an OCT structure in which the hydride ligand is located trans to the terminal phosphorus and cis to chloride, as shown by proton-coupled $^{31}P$ NMR spectra. A medium-intensity IR absorbance at 2025 $cm^{-1}$ is assigned to $\nu$(Os–H). The presence of a terminal hydride ligand is confirmed by the $^1H$ NMR spectrum, which contains a well-resolved multiplet (doublet of triplets of doublets) at –7.64 ppm. This signal can be computed as the X part of an $AMQ_2X$ spin system (Table II) with the largest coupling being between the hdyride and the trans phosphorus atom [$J(HP_{trans})$ = 75.3 Hz].

**$[(PP_3)Os(H)_2]$.** Complex **1** is converted to pale yellow crystals of the *cis*-dihydride complex $[(PP_3)Os(H)_2]$ (**3**) by treatment with a large excess (ca. 30 equiv) of $LiAlH_4$ in refluxing THF for 24 h. Decreasing either the amount of $LiAlH_4$ or the reaction time leads to the formation of mixtures of **3** and of the *cis*-hydride–chloride complex **2**.

Complex **3** is air-stable in both the solid state and deoxygenated solutions. In chlorinated solvents, a slow reaction takes place which exchanges one hydride with chloride to give **2**.

The IR spectrum of **3** contains two strong $\nu$(Os–H) absorptions at 1942 and 1827 $cm^{-1}$, which are absent in the spectrum of the perdeuterated derivative $[(PP_3)Os(D)_2]$ (**3-$d_2$**) ($K_{H/D}$ = 1.39) prepared by reacting **1** with an excess of $LiAlD_4$ in refluxing THF.

The $^{31}P\{^1H\}$ NMR spectrum shows complex **3** to be fluxional on the NMR time scale. In the fast-exchange limit ($C_6D_6$, >40 °C), the spectrum consists of an $AM_3$ spin system and transforms into an $AMQ_2$ pattern in the slow-exchange limit ($CD_2Cl_2$, <–50 °C) (Figure 1). This dynamic behavior resembles those shown by the iron $[(PP_3)Fe(H)_2]$[13] and ruthenium $[(PP_3)Ru(H)_2]$[2] analogues with the difference that the coalescence point for osmium is attained at a much higher temperature (–10 °C instead of –70 °C for ruthenium and <–100 °C for iron). At 0 °C the high-field $M_3$ portion of the spectrum collapses into a broad hump, which coalesces at ca. –10 °C. When the sample is further on cooled (–20 °C), decoalescence of the resonance takes place to give two signals (1:2 intensity ratio), which, at –50 °C, resolve into a doublet of triplets and a broad doublet, respectively. At this temperature the A portion of the spectrum appears as a broad doublet.

A satisfactory computer simulation of the variable-temperature $^{31}P\{^1H\}$ NMR spectra of **3** (DNMR3)[14] has been obtained by using $T_2$ = 0.08 s and the following rate constants $K$ ($s^{-1}$): 12 000 at 35 °C, 7000 at 20 °C, 2000 at 0 °C, 100 at –20 °C, 10 at –49 °C, and 1 at –75 °C. An Arrhenius plot of log $K$ vs $1/T$ results in a straight line from which the activation parameters $\Delta H^*$ (10.3 ± 0.8 kcal $mol^{-1}$), $\Delta S^*$ (–6 ± 3 cal $K^{-1}$ $mol^{-1}$), and thereby $\Delta G^*_{298}$ (12 ± 2 kcal $mol^{-1}$) can be calculated. An ordered transition state can be suggested on the basis of the $\Delta S^*$ value. The relatively low $E_a$ value (10.9 ± 0.8 kcal $mol^{-1}$) is consistent with the large temperature range for which a variation in the line shape is observed.

The $^1H$ NMR spectrum of **3** in $C_6D_6$ at 60 °C shows a single pseudo-doublet of quartets centered at –7.85 ppm for the two hydride ligands. This pattern, computed as the X part of an $AM_3X_2$ spin system (Table II) is interpreted in terms of coupling of instantaneously equivalent hydride ligands ($X_2$) to the trans bridgehead phosphorus atom, $P_A$, and to the three equivalent terminal phosphorus atoms, $P_M$, as unambiguously shown by selective $^1H\{^{31}P\}$ NMR experiments. Upon a decrease in the temperature, the dq resonance progressively broadens; at 30 °C a signal with no discernible coupling is observed, thus indicating that the fluxional process is on the way of being frozen out. Indeed, this resonance coalesces at 0 °C ($CD_2Cl_2$) and at –25 °C emerges from the base-line as two broad humps of equal intensity. Finally at –50 °C, the two humps resolve into a doublet of quartets of doublets and a doublet of triplets of triplets at –6.33 and –11.60 ppm, respectively (Figure 2). The splitting pattern can be regarded as the XY part of an $AMQ_2XY$ spin system. The multiplicity of the highest frequency resonance (–6.33 ppm, e.g. $H_X$) arises from coupling to the trans apical phosphorus, $P_A$, and to the three cis terminal donor atoms $P_M$ and $P_Q$ with accidentally coincident $J(H_XP_M)$ and $J(H_XP_Q)$ values. The residual coupling constant of ca. 5.2 Hz is assigned to the homonuclear $J(H_XH_{Y_{cis}})$ coupling. The coupling pattern of the lowest frequency resonance (–11.60 ppm, e.g. $H_Y$) is due to coupling to the trans terminal

(13) Bianchini, C.; Laschi, F.; Peruzzini, M.; Ottaviani, M. F.; Vacca, A.; Vizza, F.; Zanello, P. *Inorg. Chem.* **1990**, *29*, 3394.

(14) Kleiner, D. A.; Binsch, G. *A Computer Program for the Calculation of Complex Exchange-Broadened NMR Spectra; QCPE Program No. 165.*

**Table II.** Selected IR and $^1H$ NMR Spectral Data for the Complexes[a]

| compd | solvent | temp, K | δ, ppm[b] | multiplicity[c] | assgnt (intensity) | coupling const value, Hz | coupling const type[e] | ν(Os–H), cm$^{-1}$ [d] |
|---|---|---|---|---|---|---|---|---|
| **2** | $CD_2Cl_2$ | 296 | −7.64 | dtd | OsH (1 H) | 75.3 | $^2J(HP_M)$ | 2025 m |
| | | | | | | 26.7 | $^2J(HP_Q)$ | |
| | | | | | | 12.4 | $^2J(HP_A)$ | |
| **3** | $C_6D_6$ | 333 | −7.85 | p dq | $OsH_2$ (2 H) | 22.7 | $^2J(HP_A)$ | 1942 s |
| | | | | | | 8.0 | $^2J(HP_M)$ | 1827 s |
| | $CD_2Cl_2$ | 296 | −8.84 | b | $OsH_2$ (2 H) | | | |
| | | 223 | −6.33 | dqd | OsH (1 H) | 48.7 | $^2J(HP_A)$ | |
| | | | | | | −14.6 | $^2J(HP_M)$ | |
| | | | | | | −14.6 | $^2J(HP_Q)$ | |
| | | | | | | 5.2 | $^2J(HH)$ | |
| | | | −11.60 | dtt | OsH (1 H) | 55.9 | $^2J(HP_M)$ | |
| | | | | | | −28.2 | $^2J(HP_Q)$ | |
| | | | | | | −5.6 | $^2J(HP_A)$ | |
| **4** | $CD_2Cl_2/CFCl_3$ | 296 | −7.28 | b d | $OsH(H_2)$ (3 H) | 6.2 | $^2J(HP_A)$ | 2050 w |
| | | 153 | −5.68 | b | $Os(H_2)$ (2 H) | | | |
| | | | −11.20 | b | OsH (1 H) | | | |
| **4-$d_1$** | $CD_2Cl_2$ | 296 | −6.98 | q[f] | OsH(HD) (2 H)[g] | 7.5 | $^2J(HP_A)$ | |
| | | | | | | 7.5 | $^2J(HD)$[h] | |
| **4-$d_2$** | $CD_2Cl_2$ | 296 | −6.92 | s[i] | $OsH(D_2)$ (1 H)[j] | 8.3 | $^2J(HP_A)$ | |
| | | | | | | 8.3 | $^2J(HD)$[h] | |
| **5** | $CD_2Cl_2$ | 296 | −5.80 | b | OsH(HAu) (2 H) | | | 1900 w |
| | | 233 | −3.60 | dddt | Os(HAu) (1 H) | 80.4 | $^2J(HP_X)$ | |
| | | | | | | 25.4 | $^2J(HP_A)$ | |
| | | | | | | 12.6 | $^2J(HP_M)$ | |
| | | | | | | 6.5 | $^2J(HP_Q)$ | |
| | | | −8.23 | dtt | OsH(1 H) | 37.3 | $^2J(HP_M)$ | |
| | | | | | | 25.4 | $^2J(HP_Q)$ | |
| | | | | | | 13.7 | $^2J(HP_A)$ | |
| | | | | | | 13.7 | $^3J(HP_X)$ | |
| **6** | $CD_2Cl_2$ | 296 | −9.72 | dtd | OsH (1 H) | 56.1 | $^2J(HP_M)$ | 2000 m |
| | | | | | | 23.7 | $^2J(HP_Q)$ | |
| | | | | | | 15.8 | $^2J(HP_A)$ | |
| **7a** | $CD_3CN$ | 296 | −9.91 | dtd | OsH (1 H) | 64.3 | $^2J(HP_M)$ | |
| | | | | | | 26.2 | $^2J(HP_Q)$ | |
| | | | | | | 13.5 | $^2J(HP_A)$ | |
| **7b** | $CD_2Cl_2$ | 296 | −7.78 | tdd | OsH (1 H) | 30.7 | $^2J(HP_Q)$ | 2007 m |
| | | | | | | 16.6 | $^2J(HP_M)$ | |
| | | | | | | 11.8 | $^2J(HP_A)$ | |
| **7c** | TDF | 296 | −6.47 | dtd | OsH (1 H) | 55.3 | $^2J(HP_M)$ | |
| | | | | | | 26.2 | $^2J(HP_Q)$ | |
| | | | | | | 12.7 | $^2J(HP_A)$ | |
| **7d** | $CD_3COCD_3$ | 296 | −7.07 | dtd | OsH (1 H) | 72.0 | $^2J(HP_M)$ | 1960 m |
| | | | | | | 26.1 | $^2J(HP_Q)$ | |
| | | | | | | 12.1 | $^2J(HP_A)$ | |

[a] The resonances due to the hydrogen atoms of the $PP_3$ ligand are not reported. [b] Chemical shift values (δ's) are relative to tetramethylsilane as external reference. [c] Key: d, doublet; t, triplet; q, quartet; s, sextuplet; p, pseudo; b, broad. [d] Key: s, strong; m, medium; w, weak. [e] $P_A$ denotes the bridgehead phosphorus atom of the $PP_3$ ligand, whereas $P_M$ and $P_Q$ indicate the terminal donors of the same ligand. $P_X$ refers to the triphenylphosphine ligand. [f] 1:2:2:1 quartet. [g] OsH(HD) ⇔ OsD($H_2$). [h] Average value for rapidly interconverting forms. [i] 1:3:5:5:3:1 sextuplet. [j] $OsH(D_2)$ ⇔ OsD(HD).

phosphorus atom $P_M$ and to the mutually trans donor atoms $P_Q$. Finally, almost coincident values of $J(H_XH_{Y_{cis}})$ and $J(H_YP_A)$ produce the remaining triplet structure. When the sample is heated to room temperature, the starting broad signal is restored, thus showing the complete reversibility of the dynamic process.

The $^1H$ NMR fluxionality observed for complex **3** can be rationalized as due to an $AM_3X_2 \rightleftarrows AMQ_2XY$ mutual-exchange process. A satisfactory simulation of the variable-temperature spectra has been obtained by assuming that in the slow-exchange regime the coupling constants between the two hydride ligands and the corresponding trans phosphorus atom, $J(H_XP_A)$ and $J(H_YP_M)$, are plus signed while the coupling constants between the hydrides and the three cis phosphorus atoms, $J(H_XP_M)$, $J(H_XP_Q)$, $J(H_YP_A)$, and $J(H_YP_Q)$, are minus signed (see Table II).

The dynamic behavior of **3** may be related to two different processes which may also be concomitant: (i) exchange between the terminal phosphorus atoms $P_M$ and $P_Q$, that, without affecting the X part, would convert the Y multiplet to a doublet of doublets by cancellation of the inversely signed coupling constants $J(H_YP_M)$ and $J(H_YP_Q)$; (ii) exchange between the two hydride ligands that would bring to a $C_{3v}$ pseudosymmetry of the resulting dynamic structure.

The $^{31}P\{^1H\}$ and $^1H$ NMR spectra of **3** resemble those of the iron[13] and ruthenium[2] analogues $[(PP_3)M(H)_2]$ (M = Fe, Ru) for which the classical *cis*-dihydride structure was established by $T_1$ and $J$(HD) measurements. Indeed, $T_1$ experiments, carried out at 300 MHz in $CD_2Cl_2$ solution of **3** with the inversion-recovery method, gave almost coincident spin–lattice relaxation times for the terminal hydrides in the slow motion regime [210 ± 10 (low-field signal) and 200 ± 10 ms (high-field signal)]. The average $T_1$ value observed in the fast exchange regime at 25 °C is 460 ms. As observed for the ruthenium and iron analogues, these values are largely over the upper limit, which has been considered critical for the presence of a molecular hydrogen ligand.[15] On the basis of all these data and considerations, a structure can be assigned to **3** where osmium is octahedrally coordinated by the four phosphorus donors of $PP_3$ ligand and by two mutually cis hydrides.

**$[(PP_3)Os(H)(\eta^2\text{-}H_2)]BPh_4$.** Compound **3** reacts in THF solution with strong protic acids such as $HOSO_2CF_3$ to give,

(15) (a) Hamilton, D. G.; Crabtree, R. H. *J. Am. Chem. Soc.* **1988**, *110*, 4126. (b) Crabtree, R. H.; Hamilton, D. G. *Adv. Organomet. Chem.* **1988**, *28*, 299. (c) Luo, X.-L.; Crabtree, R. H. *Inorg. Chem.* **1990**, *29*, 2788. (d) Desrosiers, P. J.; Cai, L.; Lin, Z.; Richards, R.; Halpern, J. *J. Am. Chem. Soc.* **1991**, *113*, 4173.

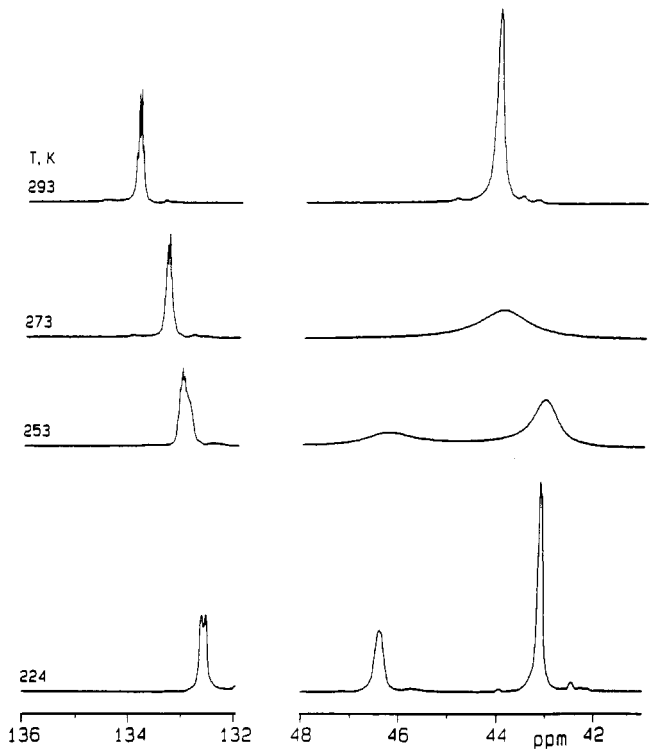


**Figure 1.** Variable-temperature $^{31}P$ NMR spectra of $[(PP_3)Os(H)_2]$ ($CD_2Cl_2$, 121.421 MHz, $H_3PO_4$ reference).

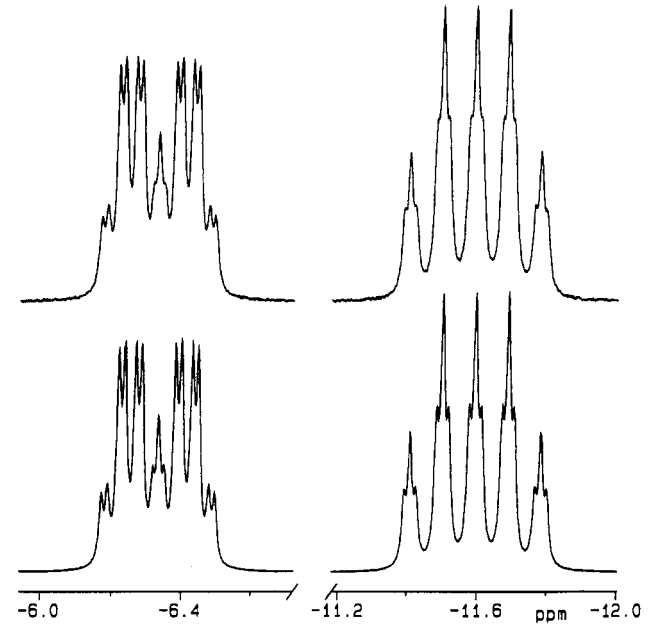


**Figure 2.** Experimental (upper) and computed (lower) $^1H$ NMR resonances of the hydride ligands in $[(PP_3)Os(H)_2]$ ($CD_2Cl_2$, -50 °C, 299.94 MHz, TMS reference).

after addition of $NaBPh_4$ and ethanol, off-white crystals of the molecular hydrogen complex $[(PP_3)Os(H)(\eta^2\text{-}H_2)](BPh_4)$ (**4**).

Compound **4** is stable in both the solid state and in solution of noncoordinating solvents, in which it behaves as a 1:1 electrolyte.

Inspection of the IR spectrum reveals no absorbance ascribable to $\nu$(H–H) or $\nu$(Os–$H_2$) vibrational modes. Actually, such absorptions are known to be very weak[16] and, in our case, as previously reported,[1,2] could also be obscured by more intense stretching vibrations of the C–C and C–H bonds of the $PP_3$ ligand. Besides the typical bands for the $BPh_4^-$ counteranion, the only informative IR absorption is a weak absorption at 2050 $cm^{-1}$ due to the terminal hydride ligand, which disappears in the spectrum of the perdeuterated isotopomer $[(PP_3)Os(D)(\eta^2\text{-}D_2)](BPh_4)$ (**4**-$d_3$) ($K_{H/D}$ = 1.42).

The $^1H$ NMR spectrum at room temperature in a 2:1 $CD_2Cl_2/CFCl_3$ mixture contains a unique resonance in the high-field region (-7.28 ppm) which appears as a broad doublet. The pattern of this signal is due to coupling of the three instantaneously equivalent hydrogen ligands to the trans bridgehead phosphorus atom as unambiguously shown by selective $^1H\{^{31}P\}$ NMR experiments. Upon a decrease in the temperature, the doublet pattern broadens and, at 0 °C, a signal with no discernible coupling is observed. This resonance coalesces at -60 °C and emerges at -110 °C from the base-line as two broad humps at -5.68 and -11.20 ppm of 2:1 relative intensity, respectively. The more intense low-field signal can be assigned to the dihydrogen ligand while the high-field resonance is assigned to the terminal hydride ligand.

Variable-temperature $T_1$ measurements carried out at 300 MHz in $CD_2Cl_2$ solutions of **4** gave a minimum spin–lattice relaxation time of 22 ± 1 ms at -40 °C. Due to the high fluxionality of the complex, the relaxation rate for the terminal hydride could not be determined. Thus, no numerical information on the H–H distance could be directly obtained.[15,17] When the fast motion regime is approached, the $T_1$ value for the exchanging hydrogens mediates to 36 ms. In the fast exchange limit, a rather low $J$(HD) coupling constant (7.5 Hz) is found for the monodeuterated isotopomer $[(PP_3)Os(H)(\eta^2\text{-}HD)]^+$ (**4**-$d_1$), which can be prepared in situ by protonation of **3** with $CF_3COOD$ ($T_{1min}$ = 32 ± 3 ms, 300 MHz, -85 °C, $CD_2Cl_2$). The observation of a small $J$(HD) is reasonably due to the rapid H/D intramolecular exchange in **4**-$d_1$ ($[(PP_3)Os(H)(\eta^2\text{-}HD)]^+ \leftrightarrows [(PP_3)Os(D)(\eta^2\text{-}H_2)]^+$). However, by using the assessment proposed by Morris and co-workers,[17b] the average $J$(HD) value (7.5 Hz) can be used to estimate a $^1J$(HD) value of ca. 22.5 Hz for the static structure. The $^1H$ NMR spectrum of **4**-$d_1$ contains a 1:2:2:1 quartet at -6.98 ppm at room temperature, which becomes a 1:1:1 deuterium triplet in the $^1H\{^{31}P\}$ NMR spectrum (Figure 3). The secondary isotopic shift of 300 ppb exhibited by this signal is larger than any other shift for $\eta^2$-HD complexes reported in the literature.[1,2,16,17]

At room temperature, the $^{31}P\{^1H\}$ NMR spectrum of **4**, in a 2:1 $CD_2Cl_2/CFCl_3$ mixture, exhibits an $AM_3$ splitting pattern, which is typical of trigonal bipyramidal (TBP) $PP_3$ complexes, including some cases of $\eta^2$-$H_2$ derivatives of $d^8$ metals.[1,2,11d,18] On decrease of the temperature, the fluxional process is progressively slowed down, until at the lowest temperature attained (-120 °C), the spectrum consists of an $AMQ_2$ pattern with no discernible $J$(PP) coupling constants (Figure 4).

The mutual-exchange mechanism that makes the terminal phosphorus atoms of $PP_3$ equivalent has been studied by DNMR3[14] spectroscopy assuming exchange between the three configurations $P_AP_MP_QP_Q \rightleftarrows P_AP_QP_MP_Q \rightleftarrows P_AP_QP_QP_M$. A satisfactory simulation of the variable-temperature spectra has been obtained by using the following rate constants $K$ ($s^{-1}$): 1 000 000 at -50 °C ($T_2$ = 0.045 s), 300 000 at -60 °C, 90 000

(16) (a) Kubas, G. J. *Acc. Chem. Res.* **1988**, *21*, 120. (b) Eckert, J.; Kubas, G. J.; Hall, J. H.; Hay, P. J.; Boyle, C. M. *J. Am. Chem. Soc.* **1990**, *112*, 2324. (c) Paciello, R. A.; Manriquez, J. M.; Bercaw, J. E. *Organometallics* **1990**, *9*, 260.

(17) (a) Bautista, M. T.; Cappellani, E. P.; Drouin, S. D.; Morris, R. H.; Schweitzer, C. T.; Sella, A.; Zubkowski, J. *J. Am. Chem. Soc.* **1991**, *113*, 4876. (b) Earl, K. A.; Jia, G.; Maltby, P. A.; Morris, R. H. *J. Am. Chem. Soc.* **1991**, *113*, 3027. (c) Collman, J. P.; Wagenknecht, P. S.; Hembre, R. T.; Lewis, N. S. *J. Am. Chem. Soc.* **1990**, *112*, 1294. (d) Ziegler, T.; Tschinke, V.; Fan, L.; Becke, A. D. *J. Am. Chem. Soc.* **1989**, *111*, 9177. (e) Harman, W. D.; Taube, H. *J. Am. Chem. Soc.* **1990**, *112*, 2261. (f) Andriollo, A.; Esteruelas, M. A.; Meyer, U.; Oro, L. A.; Sanchez-Delgado, R. A.; Sola, E.; Valero, C.; Werner, H. *J. Am. Chem. Soc.* **1989**, *111*, 7431. (g) Johnson, T. J.; Huffman, J. C.; Caulton, K. G.; Jackson, S. A.; Eisenstein, O. *Organometallics* **1989**, *8*, 2073. (h) Cappellani, E. P.; Maltby, P. A.; Morris, R. H.; Schweitzer, C. T.; Steel, M. R. *Inorg. Chem.* **1989**, *28*, 4437. (i) Amendola, P.; Antoniutti, S.; Albertin, G.; Bordignon, E. *Inorg. Chem.* **1990**, *29*, 318.

(18) Bianchini, C.; Mealli, C.; Peruzzini, M.; Zanobini, F. *J. Am. Chem. Soc.* **1987**, *109*, 5548.

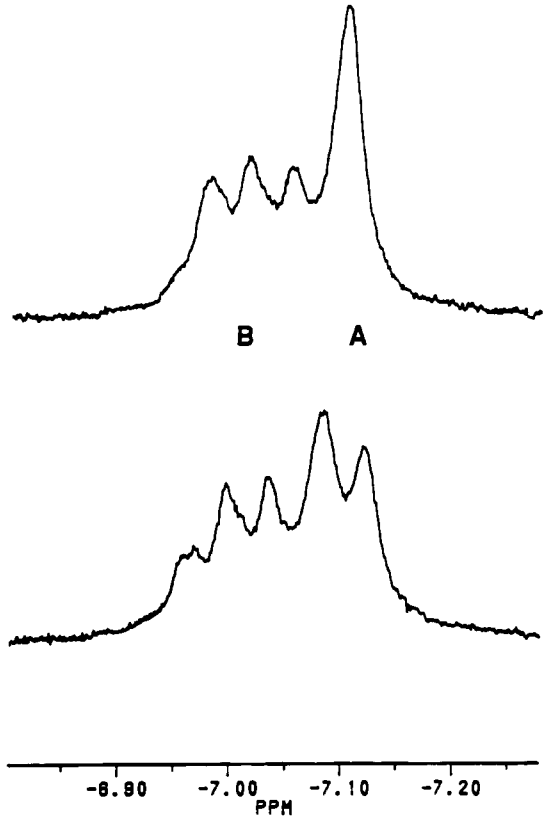


**Figure 3.** $^1H$ (lower) and $^1H\{^{31}P_A\}$ (upper) NMR spectra of a mixture of $[(PP_3)Os(H)(\eta^2\text{-}H_2)]^+$ (A) and its monodeuterated isotopomers $[(PP_3)Os(H)(\eta^2\text{-}HD)]^+$ and $[(PP_3)Os(D)(\eta^2\text{-}H_2)]^+$ (B) in the hydride region ($CD_2Cl_2$, 23 °C, 200.133 MHz, TMS reference).

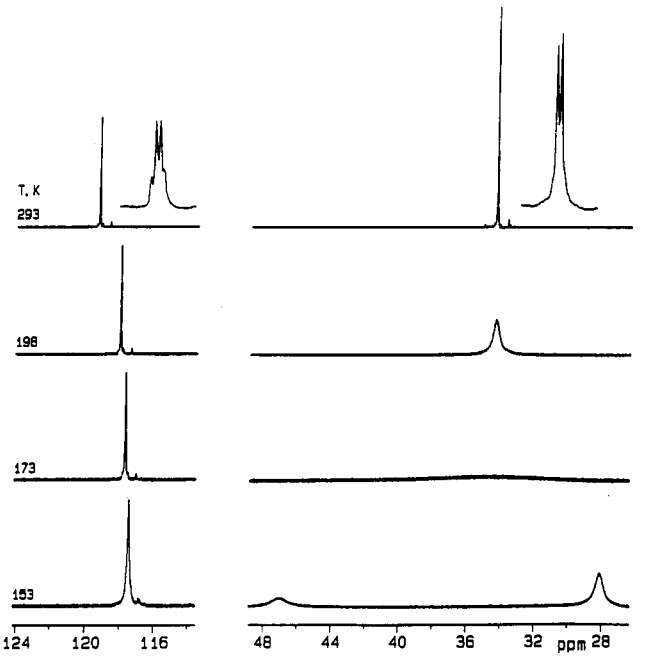


**Figure 4.** Variable-temperature $^{31}P$ NMR spectra of $[(PP_3)Os(H)(\eta^2\text{-}H_2)]BPh_4$ ($CD_2Cl_2/CFCl_3$ 2:1, 121.421 MHz, $H_3PO_4$ reference).

at −75 °C ($T_2$ = 0.044 s), 40 000 at −85 °C, 6000 at −100 °C ($T_2$ = 0.035 s), 750 at −110 °C, and 200 at −120 °C ($T_2$ = 0.016 s). Plotting log $k$ against $1/T$ results in a straight line from which the activation parameters $\Delta H^*$ (7.6 ± 0.5 kcal mol$^{-1}$) and $\Delta S^*$ (4.0 ± 3 cal K$^{-1}$ mol$^{-1}$) can be calculated. At the coalescence point, a $\Delta G^*$ value of 6.9 ± 1 kcal mol$^{-1}$ is obtained, which is appreciably smaller than those observed for the ruthenium[2] (12 ± 1 kcal mol$^{-1}$) and iron[1] (12 ± 1 kcal mol$^{-1}$) analogues. The low $E_a$ value (8.2 ± 0.5 kcal mol$^{-1}$) is consistent with the large temperature range which separates the fast-exchange and slow-exchange limits, whereas the $\Delta S^*$ value points to a relatively ordered transition state for the intramolecular exchange of the phosphorus atoms.

**Table III.** Selected Bond Distances (Å) and Angles (deg) for $[(PPh_3)Os(H)(\eta^2\text{-}H_2)]BPh_4\cdot 0.5(CH_3)_2CO$[a]

| | | | |
|---|---|---|---|
| | | Distances | |
| Os–P1 | 2.331(2) | P1–C1 | 1.844(9) |
| Os–P2 | 2.367(2) | P2–C3 | 1.845(9) |
| Os–P3 | 2.343(2) | P3–C5 | 1.85(1) |
| Os–P4 | 2.297(2) | P4–C2 | 1.807(9) |
| Os–H1 | 1.67(8) | P4–C4 | 1.84(1) |
| Os–H2 | 1.6(1) | P4–C6 | 1.817(9) |
| | | Angles | |
| P1–Os–P2 | 100.0(1) | H2–Os–P1 | 77(3) |
| P1–Os–P3 | 157.0(1) | H2–Os–P2 | 155(3) |
| P1–Os–P4 | 92.1(4) | H2–Os–P3 | 80(3) |
| P2–Os–P3 | 97.5(1) | H1–Os–H2 | 106(4) |
| P2–Os–P4 | 83.6(1) | Os–P1–C1 | 108.3(3) |
| P3–Os–P4 | 83.9(1) | Os–P2–C3 | 107.5(6) |
| H1–Os–P4 | 175(3) | Os–P3–C5 | 109.7(6) |
| H2–Os–P4 | 72(3) | Os–P4–C2 | 111.9(6) |
| H1–Os–P1 | 91(3) | Os–P4–C4 | 112.5(6) |
| H1–Os–P2 | 98(3) | Os–P4–C6 | 113.0(6) |
| H1–Os–P3 | 100(3) | | |

In order to confirm the presence of cis hydride and dihydrogen ligands in **4**, an X-ray diffraction analysis study was carried out on the compound after being recrystallized by an acetone/ethanol mixture to give **4**·0.5$(CH_3)_2CO$.

The crystal structure consists of discrete $[(PP_3)OsH_3]^+$ cations, $BPh_4^-$ anions and clathrated acetone molecules in a 1:1:0.5 ratio. A selected list of bond lengths and angles and a list of atomic coordinates for all of the non-hydrogen atoms are given in Tables III and IV, respectively. An ORTEP drawing of the complex cation is presented in Figure 5.

In keeping with the chemical–physical characterization of **4**, the coordination geometry around the Os center is an octahedron. However, the arrangement of the $PP_3$ ligand about the metal does not fully conform to the butterfly shaped which is proper of $L_4M$ fragments with $C_{2v}$ symmetry (the $P_1$–Os–$P_3$ angle of 157.0° is significatively reduced with respect to the idealized value of 180°). Quite similar distortions from the idealized geometry are commonly observed for transition metal complexes in which tetradentate tripodal ligands like $PP_3$ and $NP_3$ span two faces of an octahedron about the metal atom.[19]

A terminal hydride ligand and a "nonclassical" $H_2$ molecule are located mutually cis in the equatorial plane of the octahedron defined also by the bridgehead $P_4$ atom and by one terminal P atom of the $PP_3$ ligand ($P_2$).

The Os–P distances [2.297(2)–2.367(2) Å] fall within the range reported for osmium–phosphine complexes.[20] For comparison, the Os–P distances found in the nonclassical trihydrides *trans*-$[Os(H)(H_2)(depe)]BPh_4$ and *trans*-$[Os(H)(H_2)(dppe)]BF_4$ range from 2.328(3) to 2.357(3) Å.[21] The Os–P bond lengths in **4** are nonequivalent. The $P_2$ atom, trans to the classical hydride, exhibits the longest Os–P separation (2.367(2) Å). This finding is in agreement with previous crystallographic reports on hydride complexes containing tripodal phosphines and reflects the strong trans influence exerted by the hydride ligand.[19a–d] Likewise, since the $P_4$–Os separation is the shortest (2.297(2) Å), one may suggest a very weak trans-influence of the dihydrogen ligand. Unfor-

(19) (a) Bianchini, C.; Peruzzini, M.; Vacca, A.; Zanobini, F. *Organometallics* **1991**, *10*, 3697. (b) Di Vaira, M.; Rovai, D.; Stoppioni, P.; Peruzzini, M. *J. Organomet. Chem.* **1991**, *420*, 135. (c) Bianchini, C.; Meli, A.; Peruzzini, M.; Vizza, F.; Bachechi, F. *Organometallics* **1991**, *10*, 820. (d) Bianchini, C.; Masi, D.; Meli, A.; Peruzzini, M.; Ramirez, J. A.; Vacca, A.; Zanobini, F. *Organometallics* **1989**, *8*, 2179. (e) Linn, K.; Masi, D.; Mealli, C.; Bianchini, C.; Peruzzini, M. *Acta Crystallogr.* **1992**, *C48*, 2220.

(20) Orpen, A. G.; Brammer, L.; Allen, F. H.; Kennard, O.; Watson, D. G.; Taylor, R. *J. Chem. Soc., Dalton Trans.* **1989**, S1.

(21) (a) Earl, K. A.; Morris, R. H.; Sawyer, J. F. *Acta Crystallogr.* **1989**, *C45*, 1137. (b) Farrar, D. H.; Maltby, P. A.; Morris, R. H. *Acta Crystallogr.* **1992**, *C48*, 28.

**Table IV.** Atomic Parameters for the Structure of $[(PP_3)Os(H)(\eta^2\text{-}H_2)]BPh_4 \cdot 0.5(CH_3)_2CO$[a]

| atom | x | y | z | U or $U_{eq}$, Å$^2$ | atom | x | y | z | U or $U_{eq}$, Å$^2$ |
|---|---|---|---|---|---|---|---|---|---|
| Os1 | 1674.0(0.2) | 1779(0.2) | 4639(0.3) | 35(0)* | C2,5 | -690(4) | 738(3) | 2360(6) | 69(3) |
| H1[b] | 943(48) | 1133(53) | 5336(62) | 48(23) | C3,5 | -1477(4) | 815(3) | 1990(6) | 87(4) |
| H2 | 2205(57) | 1119(63) | 4270(73) | 74(28) | C4,5 | -1555(4) | 1637(3) | 1578(6) | 88(4) |
| P1 | 2702(1) | 1967(1) | 6107(2) | 40(1)* | C5,5 | -845(4) | 2384(3) | 1535(6) | 74(3) |
| P2 | 1349(1) | 3190(1) | 4834(2) | 40(1)* | C6,5 | -57(4) | 2307(3) | 1905(6) | 58(2) |
| P3 | 1028(1) | 1350(2) | 2866(2) | 43(1)* | C1,6 | 886(4) | 143(4) | 2369(4) | 47(2) |
| P4 | 2762(1) | 2657(2) | 3804(2) | 47(1)* | C2,6 | 740(4) | -71(4) | 1255(4) | 71(3) |
| B1 | 3634(7) | 6360(7) | 2180(9) | 49(5)* | C3,6 | 627(4) | -973(4) | 852(4) | 87(4) |
| C1 | 3678(6) | 2766(6) | 5750(7) | 53(5)* | C4,6 | 659(4) | -1662(4) | 1563(4) | 84(3) |
| C2 | 3743(5) | 2644(7) | 4538(8) | 54(5)* | C5,6 | 805(4) | -1449(4) | 2677(4) | 75(3) |
| C3 | 1903(5) | 3977(6) | 3869(7) | 49(4)* | C6,6 | 918(4) | -547(4) | 3080(4) | 58(2) |
| C4 | 2784(5) | 3878(6) | 3785(8) | 53(5)* | C1,7 | 4202(4) | 5581(4) | 2289(3) | 50(2) |
| C5 | 1735(6) | 2016(8) | 1936(7) | 60(5)* | C2,7 | 4251(4) | 5084(4) | 1351(3) | 61(3) |
| C6 | 2651(6) | 2224(7) | 2405(7) | 58(5)* | C3,7 | 4689(4) | 4429(4) | 1406(3) | 71(3) |
| C1,1 | 2582(3) | 2422(4) | 7417(4) | 46(2) | C4,7 | 5077(4) | 4270(4) | 2398(3) | 74(3) |
| C2,1 | 1879(3) | 1948(4) | 7891(4) | 54(2) | C5,7 | 5027(4) | 4767(4) | 3336(3) | 61(3) |
| C3,1 | 1778(3) | 2219(4) | 8936(4) | 72(3) | C6,7 | 4589(4) | 5423(4) | 3282(3) | 51(2) |
| C4,1 | 2379(3) | 2963(4) | 9506(4) | 77(3) | C1,8 | 3898(3) | 6928(5) | 1059(5) | 54(2) |
| C5,1 | 3082(3) | 3437(4) | 9031(4) | 76(3) | C2,8 | 3295(3) | 7035(5) | 256(5) | 67(3) |
| C6,1 | 3184(3) | 3166(4) | 7987(4) | 57(2) | C3,8 | 3537(3) | 7459(5) | -688(5) | 85(3) |
| C1,2 | 3038(4) | 944(4) | 6495(4) | 42(2) | C4,8 | 4381(3) | 7775(5) | -828(5) | 88(4) |
| C2,2 | 2915(4) | 191(4) | 5761(4) | 59(3) | C5,8 | 4984(3) | 7668(5) | -25(5) | 73(3) |
| C3,2 | 3223(4) | -543(4) | 6051(4) | 70(3) | C6,8 | 4743(3) | 7244(5) | 918(5) | 66(3) |
| C4,2 | 3654(4) | -523(4) | 7076(4) | 73(3) | C1,9 | 2604(4) | 5840(4) | 2017(5) | 56(2) |
| C5,2 | 3778(4) | 230(4) | 7810(4) | 76(3) | C2,9 | 2273(4) | 5048(4) | 1326(5) | 59(3) |
| C6,2 | 3470(4) | 964(4) | 7520(4) | 57(2) | C3,9 | 1410(4) | 4665(4) | 1106(5) | 73(3) |
| C1,3 | 1635(3) | 3898(4) | 6126(5) | 49(2) | C4,9 | 877(4) | 5075(4) | 1577(5) | 86(3) |
| C2,3 | 1102(3) | 3653(4) | 6924(5) | 60(3) | C5,9 | 1208(4) | 5868(4) | 2267(5) | 90(4) |
| C3,3 | 1271(3) | 4180(4) | 7903(5) | 73(3) | C6,9 | 2071(4) | 6250(4) | 2487(5) | 73(3) |
| C4,3 | 1972(3) | 4952(4) | 8083(5) | 79(3) | C110 | 3909(4) | 7076(4) | 3298(5) | 53(2) |
| C5,3 | 2505(3) | 5198(4) | 7285(5) | 73(3) | C210 | 3641(4) | 6715(4) | 4261(5) | 72(3) |
| C6,3 | 2336(3) | 4670(4) | 6306(5) | 61(3) | C310 | 3918(4) | 7246(4) | 5234(5) | 86(4) |
| C1,4 | 269(4) | 3188(3) | 4518(5) | 45(2) | C410 | 4462(4) | 8138(4) | 5245(5) | 86(4) |
| C2,4 | -375(4) | 2394(3) | 4655(5) | 58(2) | C510 | 4729(4) | 8500(4) | 4283(5) | 84(3) |
| C3,4 | -1204(4) | 2403(3) | 4473(5) | 76(3) | C610 | 4453(4) | 7968(4) | 3309(5) | 67(3) |
| C4,4 | -1389(4) | 3205(3) | 4155(5) | 78(3) | C7 | 3897(19) | -319(21) | 982(25) | 107(9) |
| C5,4 | -745(4) | 3999(3) | 4018(5) | 76(3) | C8 | 3606(14) | -4(16) | 1988(18) | 69(6) |
| C6,4 | 84(4) | 3990(3) | 4200(5) | 63(3) | C9 | 3078(22) | -628(24) | 2519(28) | 125(11) |
| C1,5 | 20(4) | 1484(3) | 2317(6) | 47(2) | O1 | 3955(14) | 702(16) | 2380(18) | 128(7) |

[a] Note: Thermal parameters multiplied by 1000, and coordinates by 10000. An asteisk denotes $U_{eq}$ defined as one-third of the trace of the orthogonalized thermal tensor. [b] The atom reported as H1 is most likely the crystallographic image of an unresolved $H_2$ molecule trans to the atom $P_4$ (as other spectroscopic data suggest). The coordinates of H1 were refined in the least-squares cycles.

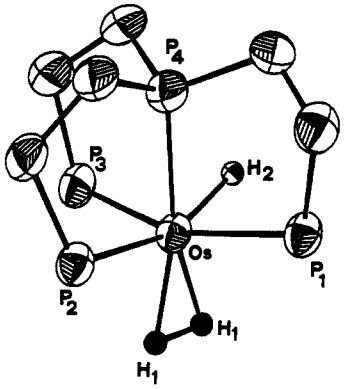


**Figure 5.** ORTEP drawing of the complex cation $[(PP_3)OsH((\eta^2\text{-}H_2)]^+$. The two atoms of the $\eta^2$-$H_2$ ligand are presented as darkened spheres in an hypothetical position based on the spectroscopical information. Crystallographically, the two H atoms appear as an unique unresolved peak.

tunately, a comparison with other $M(H)(\eta^2\text{-}H_2)$ complexes containing phosphorus donors trans to the H and $H_2$ ligands is precluded for the lack of X-ray-authenticated molecular hydrogen complexes of the present type.

The Os–H terminal distance, 1.6(1) Å, is similar to that pertaining to the nonclassical ligand [1.67(8) Å] and falls within the range reported by Orpen and co-workers [Os–$H_{av}$ = 1.659 Å, $\sigma$ = 0.017].[20] However, we honestly recognize that the quality of the present crystallographic study does not allow one to discuss the Os–$H_2$ bond. In fact, the refinement procedure of the structure did not meet complete success. At an advanced stage of the structure refinement, two intensities of ca. 0.6 $e^-/Å^3$ in the Fourier difference map were taken into account and considered, in keeping with the spectroscopic analysis, as hydrogen atoms bonded to osmium. The refinement procedure clearly confirmed the presence of two "hydride" ligands and was succesfully retained. However, while there is no doubt that the hydride trans to the terminal phosphorus atom $P_2$ is the classical one, it was not possible to separate the other electron-density spot into the two H components of the nonclassical $H_2$ ligand molecule. This was just introduced in a calculated position assuming an H–H separation of ca. 0.95 Å, i.e. the value figured out from $T_{1(min)}$ (see above).

Di- and trideuterated isotopomers of **4**, $[(PP_3)Os(H)(\eta^2\text{-}D_2)]^+$ or $[(PP_3)Os(D)(\eta^2\text{-}HD)]^+$ (**4**-$d_2$) and $[(PP_3)Os(D)(\eta^2\text{-}D_2)]^+$ (**4**-$d_3$), were also synthesized in situ by protonation of $[(PP_3)Os(D)_2]$ (**3**-$d_2$) with $CF_3COOH$ and $CF_3COOD$, respectively. In the proton NMR spectrum ($CD_2Cl_2$), compound **4**-$d_2$ shows a 1:3:5:5:3:1 sextuplet at –6.92 ppm at room temperature. The pattern of this signal is originated by coupling of the H nucleus to the two deuterium atoms [$J$(HD) = 8.3 Hz] which are made equivalent by the exchange process, and to the trans bridgehead phosphorus atom, with a $J(HP_A)$ value of approximately the same magnitude. $^{31}P$ NMR data for **4**-$d_1$, **4**-$d_2$, and **4**-$d_3$ are reported in Table I.

**$[(PP_3)Os(H)\{\eta^2\text{-}HAu(PPh_3)\}]PF_6$.** Stirring the dihydride complex **3** in THF with a slight excess of $[AuCl(PPh_3)]$ in the presence of $[NH_4]PF_6$ produces a colorless solution from which crystals of $[(PP_3)Os(H)\{\eta^2\text{-}HAu(PPh_3)\}]PF_6$ (**5**) can be obtained

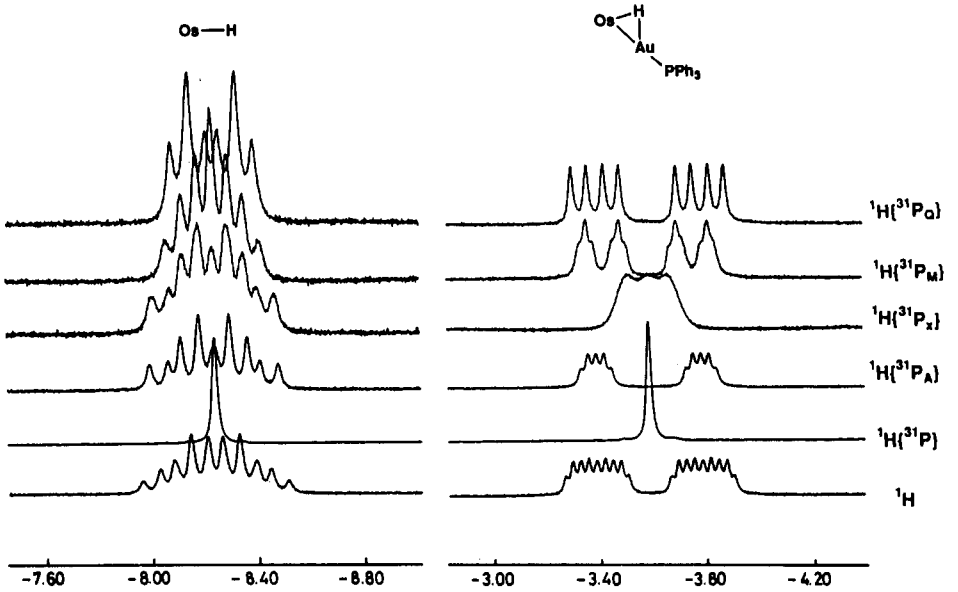


**Figure 6.** $^1H$ and selective $^1H\{^{31}P\}$ spectra of $[(PP_3)Os(H)(\eta^2\text{-}HAu(PPh_3))]PF_6$ ($CD_2Cl_2$, −50 °C, 200.133 MHz, TMS reference).

in 80% yield. Complex **5** appears as cream colored crystals and is stable in both the solid state and solution in which it behaves as a 1:1 electrolyte.

In addition to the typical bands of the $PF_6^-$ counteranion and of the $PP_3$ ligand, the IR spectrum contains a weak $\nu$(Os–H) absorption at 1900 $cm^{-1}$. Variable-temperature $^{31}P\{^1H\}$ NMR spectra in $CD_2Cl_2$ show complex **5** to be highly fluxional on the NMR time scale. In the fast-exchange limit (>30 °C) the spectrum consist of an $AM_3X$ spin system which transforms into an $AMQ_2X$ pattern in the slow-exchange limit (<−35 °C) with a coalescence temperature of −15 °C for the $M_3$ portion. When the dynamic process is frozen out the chemical shifts and coupling constants of the $AMQ_2$ portion of the spectrum are quite similar to those observed for all $PP_3$ osmium complexes herein described (Table I). Also, the relatively large value of the coupling constant $J(P_AP_X)$ (28.9 Hz at −40 °C) is consistent with a transoid arrangement of the $PPh_3$ ligand and of the bridgehead phosphorus $P_A$.[9j,22]

The $^1H$ NMR spectrum at room temperature contains a unique broad resonance in the hydride region at −5.80 ppm, thus indicating rapid exchange of the two hydride ligands. Upon a decrease in the temperature, this resonance coalesces and emerges from the baseline at 0 °C as two broads humps of equal intensity. Finally, at −40 °C, both humps resolve (Figure 6) into fine structure: $\delta$ −6.30 (doublet of doublets of doublets of triplets, $T_1$ = 210 ± 5 ms), $\delta$ −8.23 (doublet of triplets of triplets, $T_1$ = 210 ± 5 ms). The dynamic process is fully reversible. The low-field signal is readily assigned to a bridging hydride for its chemical shift and the large $J(HP_X)$ coupling constant unambiguosly determined by means of selective-decoupling $^1H\{^{31}P\}$ NMR experiments. Likewise, the $J(HP_A)$, $J(HP_M)$, and $J(HP_Q)$ coupling constants are consistent with a mutual transoid arrangement of the bridging hydride and of the bridgehead phosphorus $P_A$.[9j,22]

The high-field resonance is therefore assigned to a terminal hydride ligand. The fortuitous coincidence of the $^2J(HP_X)$ and $^3J(HP_M)$ values (Table II) is responsible for the observed dtt multiplicity.

In light of the spectroscopic data, an octahedral structure can be assigned to **5** in which the terminal hydride ligand is located trans to the terminal phosphorus $P_M$ and the dihapto-bonded "$[HAu(PPh_3)]^+$" moiety is transoid to the bridgehead phosphorus $P_A$. Noteworthy, an identical primary geometry has been found for the $\eta^2$-$H_2$ derivative **4**.

(22) Mueting, A. M.; Bos, W.; Alexander, B. D.; Boyle, P. D.; Casalnovo, J. A.; Balaban, S.; Ito, L. N.; Johnson, S. M.; Pignolet, L. H. *New J. Chem.* **1988**, *12*, 505.

The isolobal relationship of $H^+$ and $[Au(PR_3)]^+$ is being throughly used in metal cluster chemistry to visualize the hydride position.[9] Indeed, in almost all compounds containing one $[Au(PR_3)]^+$ group and where structural comparisons are possible, the $[Au(PR_3)]^+$ fragment occupies a position similar to that of the hydride ligand into related hydrido metal clusters. Recently, the isolobal analogy concept has been extended to H–H, Au–H, and Au–Au systems, namely $H_2$ is isolobal with $[Au_2(PR_3)_2]$, $H_3^+$ is isolobal with $[Au_3(PR_3)_3]^+$, and $H_2$ is isolobal with $HAu(PR_3)$.[9] The isolation and characterization of **5**, thus, provides further experimental evidence of the correctness of this theoretical approach.

**$[(PP_3)Os(H)(N_2)]BPh_4$.** The reaction between **3** and a stoichiometric amount of $CH_3OSO_2CF_3$ in THF under nitrogen yields lemon yellow crystals of $[(PP_3)Os(H)(N_2)](BPh_4)$ (**6**) after addition of $NaBPh_4$ and ethanol. Evolution of methane was detected by GC.

Complex **6** is fairly air-stable in the solid state and in solutions of noncoordinating solvents under $N_2$. In coordinating solvents such as $CH_3CN$ ($N_2$ atmosphere) or THF (argon atmosphere), **6** rapidly converts to the corresponding solvento complex, $[(PP_3)Os(H)(solvent)]^+$ (solvent = $CH_3CN$, **7a**; THF, **7c**), as shown by in situ NMR experiments (see below).

The IR spectrum of **6** shows a strong absorption at 2144 $cm^{-1}$, which can be assigned to $\nu(N{\equiv}N)$, while a medium-intensity band at 2000 $cm^{-1}$ is ascribable to $\nu$(Os–H).[1,2] Complex **6** exhibits a temperature-invariant pseudo-first-order $^{31}P\{^1H\}$ NMR $AMQ_2$ spin system in $CD_2Cl_2$ with a moderate second-order component. The presence of a terminal hydride ligand is confirmed by the $^1H$ NMR spectrum, which contains a doublet of triplets of doublets at −9.72 ppm. Again, selective decoupling experiments allowed us to unambiguosly assign all resonances and $J$(HP) values, and, thus, an OCT structure to **6** in which the terminal hydride ligand is located trans to the terminal phosphorus $P_M$ and cis to the dinitrogen ligand.

**$[(PP_3)Os(H)(L)]BPH_4$ (L = $CD_3CN$ (7a), CO (7b), THF-$d_8$ (7c), $CH_3COCH_3$ (7d)).** Compound **4** is stable for hours in coordinating solvents ($CH_3CN$, THF, acetone) at room temperature under nitrogen atmosphere. Substitution of acetonitrile for $H_2$ takes place at high temperatures (>50 °C, 30 min) to give the OCT monohydrido adduct $[(PP_3)Os(H)(NCCH_3)]^+$. The use of high temperatures to displace the $H_2$ ligand is necessary also for the reactions with strong ligands such as CO, which displaces $H_2$ only in refluxing THF to give $[(PP_3)Os(H)(CO)]BPh_4$ (**7b**). This behavior markedly contrasts with that of the ruthenium analogue,[2] which easily undergoes displacement of

the dihydrogen ligand by other neutral ligands in room-temperature solutions. Compound **4** is even more stable than the iron analogue, which, although very slowly, is transformed into the corresponding $N_2$, $CH_3CN$, or CO derivatives in room-temperature solutions.[1]

The Os–$H_2$ bond, thus, appears abnormally strong, a fact that is supported also by the nonoccurrence of H/D exchange reactions in $CD_2Cl_2$ with $D_2$ even for long reaction times (12 h). In contrast, H/D isotope exchange reactions can be achieved by using deuterated solvents such as $CD_3OD$, $D_2O$, or, surprisingly, $CD_3COCD_3$ (see forthcoming pages).

Quite different behavior is shown by **6** which readily undergoes displacement of the $N_2$ ligand at room temperature by a variety of molecules, including those with weak donating properties. As an example, the complex reacts with THF and $CH_3COCH_3$ to give $[(PP_3)Os(H)(THF)]^+$ (**7c**) characterized in situ by NMR spectroscopy and $[(PP_3)Os(H)\{\eta^1\text{-}OC(CH_3)_2\}]BPh_4$ (**7d**) isolated in the solid state as pale yellow crystals.

As expected, the displacement of dinitrogen by dihydrogen is an immediate and irreversible reaction.

The presence of terminal hydride ligand in complexes **7a–d** is shown by IR and $^1H$ NMR spectra (Table II). The IR spectrum of **7b** contains also a strong absorption at 1947 $cm^{-1}$ ascribable to $\nu$(CO), while the spectrum of **7d** exhibits a band at 1652 $cm^{-1}$ which can reasonably be assigned to the $\nu$(CO) vibrational mode of an $\eta^1$-*O*-acetone complex.[23] In keeping with the presence of an oxygen-bonded acetone molecule, the $^{13}C\{^1H\}$ NMR spectrum of **7d** in $CD_2Cl_2$ shows the carbonyl (223.0 ppm) and methyl (31.4 ppm) resonances low-field shifted with respect to free acetone.[23,24] Finally, the $^1H$ NMR spectrum exhibits a singlet at 1.84 ppm (6 H) assigned to the $CH_3$ hydrogens of the coordinated acetone.

Although some $\eta^1$- and $\eta^2$-ketone complexes have been reported in the literature, mainly by Gladysz and co-workers,[25] only one example of a stable cis-hydride–$\eta^1$-ketone complex has been described so far.[10b] Compounds of the latter type have often been proposed to play a key role in the catalytic reduction of aldehydes and ketones to the corresponding alcohols.[10]

All $^{31}P\{^1H\}$ NMR spectra of **7a–d** consist of first-order $AMQ_2$ splitting patterns (some second-order component is observed for **7a** at 81.015 MHz) (Table I).

**H/D Isotope Exchange Reactions between 4 and $D_2O$, $CD_3OD$, and $CD_3COCD_3$.** Compound **4** in $CD_2Cl_2$ readily exchanges its H atoms with deuterium by reaction with an excess of either $D_2O$ or $CD_3OD$ at room temperature. The isotope exchange reactions are very fast and quantitatively produce the perdeuterated isotopomer **4**-$d_3$, as shown by the disappearance of any $^1H$ NMR resonance in the hydride region. In contrast, all isotopomers of **4** (**4**-$d_1$, **4**-$d_2$, **4**-$d_3$) can be observed upon dissolution of complex in $CD_3COCD_3$. All isotopomers can be also detected by NMR spectroscopy when a solution of the perdeuterated complex is dissolved in $CH_3COCH_3$.

The H/D exchange reaction with acetone is much slower than those with deuterated water or methanol. Complete deuteration of **4** to **4**-$d_3$ takes place in several hours with a rate that is proportional to the initial concentration of the complex. The perdeuterated isotopomer **4**-$d_3$ can be isolated by addition of dry *n*-heptane.

No chemical reaction occurs between **4** and acetone even at reflux temperature indicating that the $H_2$ ligand is not displaced by acetone to give the acetone adduct **7**-*d* that we have shown to be a stable and isolable compound. Variable-temperature $^{31}P\{^1H\}$ NMR spectra of **4** in $CD_3COCD_3$ from –80 to 45 °C show that all four phosphorus atoms of $PP_3$ remain coordinated to the metal during the H/D exchange reaction. There was no evidence for deuterium incorporation into the $PP_3$ ligand or for $H_2$ evolution during all the isotope exchange reactions, which occur even at low temperature (–50 °C). Finally, it is interesting to note that neither the hydride–dinitrogen derivative **6** nor the $\eta^2$-HAu($PPh_3$) dihydride **5** undergo H/D exchange by treatment with $D_2O$, $CD_3OD$, or $CD_3COCD_3$.

## Discussion

**The $[(PP_3)MH(\eta^2\text{-}H_2)]BPh_4$ Family.** A comparison within the series of $PP_3$ *cis*-hydride–$\eta^2$-dihydrogen complexes readily shows that the trend in spectroscopic and chemical properties down the iron group triad is qualitatively similar to that observed by Morris and co-workers for the related family of *trans*-hydride–$\eta^2$-dihydrogen compounds $[M(H)(\eta^2\text{-}H_2)L_2]$ stabilized by the dppe and depe ligands.[8] In particular, the Ru complexes have the weakest interaction with the $H_2$ ligand, a fact that inelastic neutron scattering experiments on the $PP_3$ derivative have related to a weaker back-bonding capability of Ru.[7]

In light of the $\nu$(N≡N),[26] $J$(HD), and $T_1$ values, the H–H bond distance in the Os complex is expected to be the largest in the $PP_3$ series. As nicely demonstrated by Morris,[8] the remarkable strength of the Os–$H_2$ bond is due to the greater $\sigma$-bond energy than that of the corresponding Fe derivative and greater $\sigma$- and $\pi$-energies than those of the Ru complex. However, it is worth stressing that the overall stability of the $PP_3$ complexes is much higher than that of the corresponding depe and dppe compounds. Such a difference in stability may be explained in terms of an attractive "cis-effect" of hydride on neighbor dihydrogen (stabilizing overlap between the filled Fe–H $\sigma$ orbital and the empty $\sigma^*_{H-H}$), as suggested by Caulton, Eisenstein, and co-workers for $[Fe(H)_2(\eta^2\text{-}H_2)(PEtPh_2)_3]$.[27] Also, these investigators proposed that the cis-effect can facilitate the $H/H_2$ fluxionality of the complex by avoiding an intermediate with four independent hydride ligands. Within this context, it is not accidental that all *cis*-H–$\eta^2$-$H_2$ complexes of $PP_3$ are much more fluxional than the corresponding depe and dppe derivatives.

In previous papers, based on the computer simulation of the $^{31}P$ NMR spectra, we interpreted the dynamic behavior of the Fe and Ru complexes of $PP_3$ as involving a transition state with either a closed or open trihydrogen moiety.[1,2] Interestingly, Bertrán and co-workers have more recently reported an ab initio theoretical study on the intramolecular reaction involving exchange of hydrogen atom between cis hydride and dihydrogen ligands in the model system *cis*-$[Fe(PH_3)_4H(H_2)]^+$.[28] Of the three possible mechanisms shown in Scheme II, the open direct transfer results as the most favored, with an energetic barrier of only 3.2 kcal $mol^{-1}$. Indeed, a mechanism of this type may be operative for the fluxional process exhibited by the Os complex **4**, for which quite consistent activation parameters, particularly $\Delta S^*$, have been found.

**H/D Isotope Exchange Reactions.** Dihydrogen metal complexes are being currently used as catalysts for H/D exchange between protic solvents and $D_2$, due to their Brønsted acidity and the rapid reversible dissociation of $H_2$.[29a] In contrast, very few examples of H/D exchange between $\eta^2$-$H_2$ complexes and aprotic

(23) Brown, J. M.; Chaloner, P. A. *J. Chem. Soc., Perkin Trans.* **1982**, *2*, 711.
(24) Dean Harman, W.; Fairlie, D. P.; Taube, H. *J. Am. Chem. Soc.* **1986**, *108*, 8223.
(25) (a) Agbossou, F.; Ramsden, J. A.; Huang, Y.-H.; Arif, A. M.; Gladysz, J. A. *Organometallics* **1992**, *11*, 693 and references therein. (b) Gladysz, J. A. Presented at the XVth International Conference on Organometallic Chemistry, Warsaw, Poland, August 9–14, 1992; Abstract PL5.
(26) Morris, R. H.; Earl, K. A.; Luck, R. L.; Lazarowych, N. J.; Sella, A. *Inorg. Chem.* **1987**, *26*, 2674.
(27) (a) Van Der Sluys, L. S.; Eckert, J.; Eisenstein, O.; Hall, J. H.; Huffman, J. C.; Jackson, S. A.; Koetzle, T. F.; Kubas, G. J.; Vergamini, P. J.; Caulton, K. G. *J. Am. Chem. Soc.* **1990**, *112*, 4831. (b) Riehl, J.-L.; Pélissier, M.; Eisenstein, O. *Inorg. Chem.* **1992**, *31*, 3344. (c) Riehl, J.-F.; Jackson, S. A.; Pélissier, M.; Eisenstein, O. *Bull. Soc. Chim. Fr.* **1992**, *129*, 221.
(28) Maseras, F.; Duran, M.; Lledós, A.; Bertrán, J. *J. Am. Chem. Soc.* **1992**, *114*, 2922.
(29) (a) Albeniz, A. C.; Heinekey, D. M.; Crabtree, R. H. *Inorg. Chem.* **1991**, *30*, 3632. (b) Mediati, M.; Tachibana, G. N.; Jensen, M. C. *Inorg. Chem.* **1992**, *31*, 1827. (c) Bautista, M. T.; Earl, K. A.; Maltby, P. A.; Morris, R. H. *J. Am. Chem. Soc.* **1988**, *110*, 4056.

**Scheme II**

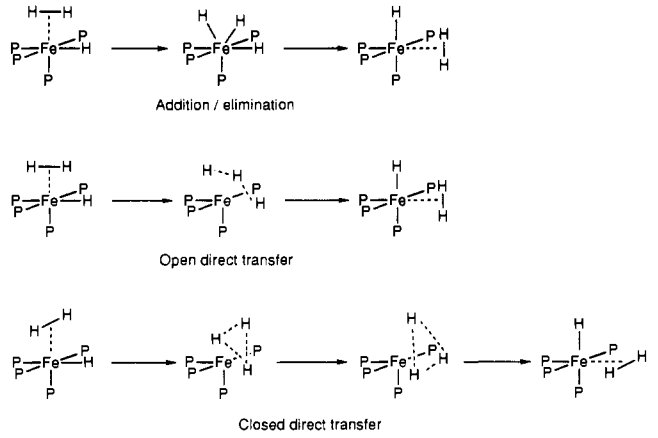


**Scheme III**

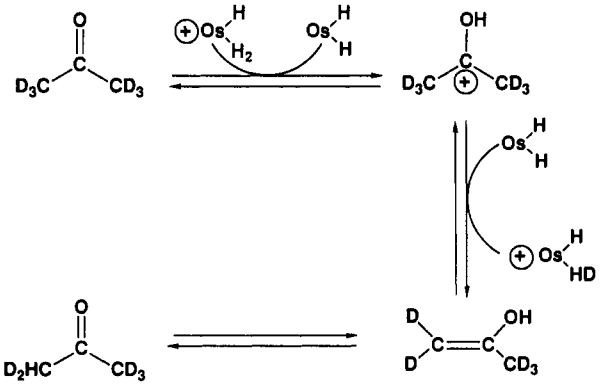

solvents have been reported, while no mechanistic interpretation has even been proposed.[29b,c]

Since the $H_2$ ligand in **4** is strongly bound to the metal center to the extent that it does not exchange with $D_2$ in solution, one can reasonably conclude that the reaction with acetone-$d_6$ does not proceed via $H_2$ decoordination at any stage. On the other hand, we did not observe $H_2$ evolution during the H/D exchange.

The experimental evidence accumulated for the reaction, particularly the observation that neither the hydride–dinitrogen complex **6** nor the $\eta^2$-HAu($PPh_3$) dihydride **5** incorporate deuterium by treatment with acetone-$d_6$, leads to the conclusion that the $\eta^2$-$H_2$ ligand in **4** plays a crucial role in the H/D exchange reaction. Actually, **4** is somewhat acidic being deprotonated to the neutral dihydride **3** in THF solution by both $t$-$BuO^-$ ($pK_a$ 18) and $EtO^-$ ($pK_a$ 16), but not by $NEt_3$ ($pK_a$ 11). By using Morris' method,[30] the predicted $pK_a$ value of **4** spans over 18 $pK_a$ units (from 10 to 28). However, the real value should be closer to 12–15 since an experimental value of 12.6 (extrapolated to aqueous scale) has been reported for the related dppe derivative [OsH-($\eta^2$-$H_2$)(dppe)]$BF_4$.[30]

In conclusion, one may reasonable state that the Os complex **4** is more acidic than acetone, which exhibits a $pK_a$ value of 20.[31] If so, the isotope exchange reaction may proceed via a keto–enol tautomerization of acetone catalyzed by **4**, as shown in Scheme III.

The proposed mechanism involves a proton transfer from **4** to acetone-$d_6$. As a result, the dihydride **3** forms, which, by extraction of deuterium from the resulting carbocation, converts to **4**-$d_1$ (an equilibrium mixture of $[(PP_3)OsH(\eta^2\text{-}HD)]^+$ and $[(PP_3)OsD(\eta^2\text{-}H_2)]^+$). Interaction of the latter species most likely with another acetone-$d_6$ molecule, of which there is large excess, may then afford **4**-$d_2$. As the process goes on, all **4** is eventually converted to **4**-$d_3$.

Provided the mechanism shown in Scheme III is valid, the isotope exchange reactions between **4** and $D_2O$ ($pK_a$ 14) and $CD_3OD$ ($pK_a$ 15.5) can also be explained in terms of a deprotonation/reprotonation pathway of the acid–base couple **4**–**3**.

## Experimental Section

**Reagents.** $[OsCl_2(PPh_3)_3]$ and $[AuCl(PPh_3)]$ were synthesized as described by Elliot et al.[32] and Bruce et al.,[33] respectively. The $PP_3$ ligand was purchased from Pressure Co. and used without further purification. Tetrahydrofuran and dichloromethane were purified by distillation over $LiAlH_4$ and $P_2O_5$ under nitrogen just prior to use, respectively. All the other solvents and chemicals were reagent grade and were used as received by commercial suppliers.

**Spectroscopics Measurements.** Infrared spectra of samples mulled in Nujol between KBr plates were recorded on a Perkin-Elmer 1600 Series FTIR spectrophotometer. Deuterated solvents for NMR measurements were dried over molecular sieves. Proton NMR spectra were recorded at 299.94 and 200.13 MHz on Varian VXR 300 and Bruker ACP 200 spectrometers, respectively. Peak positions are relative to tetramethylsilane as external reference. $^{31}P\{^1H\}$ NMR spectra were recorded on the same instruments operating at 121.42 and 81.01 MHz, respectively. Chemical shifts are relative to external 85% $H_3PO_4$, with downfield values reported as positive. Broad-band and selective $^1H\{^{31}P\}$ NMR experiments were carried out on the Bruker ACP 200 instrument equipped with a 5-mm inverse probe and a BFX-5 amplifier device.

**Computer Simulations of the NMR Spectra.** The computer simulation of NMR spectra was carried out with a locally developed package containing the programs LAOCN3[34] and DAVINS[35] run on a Compaq Deskpro 386/25 personal computer. The initial choices of shifts and coupling constants were refined by iterative least-squares calculations using the experimental digitized spectrum. The final parameters gave a satisfactory fit between experimental and calculated spectra, the agreement factor $R$ being less than 1% in all cases.

The line shape analysis of the variable-temperature NMR spectra was accomplished by means of the DNMR3 program[14] adapted for the Compaq computer. Errors in the calculated rate constants were estimated by varying the rate constant around the best-fit value, until no observable difference between simulated and experimental spectra, both displayed on the graphical terminal, could be detected. These errors proved to be 5% or less.

**Conductivity Measurements.** Conductivities were measured with an ORION Model 990101 conductance cell connected to a Model 101 conductivity meter. The conductivity data were obtained at sample concentrations of ca. $1 \times 10^{-3}$ M in nitroethane solutions at room temperature (20 °C).

**Synthesis of the Complexes.** All reactions and manipulations were routinely performed under a dry nitrogen or argon atmosphere by using Schlenk-tube techniques. The solid compounds were collected on sintered-glass frits and washed with ethanol and petroleum ether (bp 50–70 °C) before being dried in a stream of nitrogen.

**Preparation of $[(PP_3)OsCl_2]$ (1).** A 2.10 g (2.00 mmol) sample of $[OsCl_2(PPh_3)_3]$ and 1.40 g (2.00 mmol) of $PP_3$ were dissolved in 150 mL of 2-methoxyethanol, and the solution was heated to reflux temperature. The reflux was maintained for 3 h, and then the volume was reduced by distillation to ca. 20 mL. Addition of ethanol (50 mL) gave **1** as a cream colored crystals. The precipitation of **1** was completed by cooling the mixture down to 0 °C by means of an ice bath. The crude product was purified by recrystallization from $CH_2Cl_2$/EtOH (yield 75%). Anal. Calcd for $C_{42}H_{42}Cl_2OsP_4$: C, 54.14; H, 4.54; Cl, 7.61. Found: C, 53.98; H, 4.49; Cl, 7.54.

**Preparation of $[(PP_3)OsHCl]$ (2).** Neat $LiHBEt_3$ (0.60 mL of a 1 M THF solution, 0.60 mmol) was syringed into a THF (25 mL) solution of **1** (0.50 g, 0.54 mmol) to produce a clear yellow solution that deposited pale yellow crystals of **2** after addition of ethanol (30 mL). Yield: 90%. Anal. Calcd for $C_{42}H_{43}ClOsP_4$: C, 56.22; H, 4.83; Cl, 3.95. Found: C, 56.13; H, 4.80; Cl, 3.79.

**Preparation of $[(PP_3)Os(H)_2]$ (3).** Solid $LiAlH_4$ (1.10 g, 29.02 mmol) was added portionwise to a stirred suspension of **1** (1.00 g, 1.07 mmol) in 150 mL of THF. The mixture was heated to reflux temperature and

(30) Morris, R. H. *Inorg. Chem.* **1992**, *31*, 1471.
(31) Dean Harman, W.; Sekine, M.; Taube, H. *J. Am. Chem. Soc.* **1988**, *110*, 2439.
(32) Elliott, G. P.; Mcauley, N. M.; Roper, W. R. *Inorg. Synth.* **1989**, *26*, 184.
(33) Bruce, M. I.; Nicholson, B. K.; Bin Shawkataly, O. *Inorg. Synth.* **1989**, *26*, 325.
(34) Castellano, S.; Bothner-By, A. A. *J. Chem. Phys.* **1964**, *41*, 3863.
(35) Stephenson, D. S.; Binsch, G. *J. Magn. Reson.* **1980**, *37*, 395.

stirred for 24 h. The reaction vessel was then cooled to 0 °C and the excess of $LiAlH_4$ hydrolyzed by careful addition of a mixture of THF/$H_2O$ (50 mL, 3:1 v/v). The resulting slurry was filtered to remove the lithium and aluminum hydrolysis products. The volume of the filtrate was reduced by distillation to ca. 40 mL. By addition of ethanol (50 mL), followed by slow concentration in a stream of nitrogen, pale yellow crystals of **3** separated (yield 80%). Anal. Calcd for $C_{42}H_{44}OsP_4$: C, 58.46; H, 5.14. Found: C, 58.35; H, 5.03.

The perdeuterated derivative $[(PP_3)Os(D)_2]$ (**3-$d_2$**) was prepared in 95% yield ($^1H$ NMR) by substituting $LiAlD_4$ and $C_2H_5OD$ for $LiAlH_4$ and $C_2H_5OH$ in the above procedure.

**Preparation of $[(PP_3)Os(H)(\eta^2\text{-}H_2)]BPh_4$ (4).** Neat $HOSO_2CF_3$ (0.08 mL, 0.91 mmol) was syringed into a THF suspension (10 mL) of **3** (0.60 g, 0.70 mmol) under $H_2$ atmosphere. The mixture was stirred for 30 min, during which time the starting product dissolved to give a colorless solution. Addition of $NaBPh_4$ (0.40 g, 1.17 mmol) and ethanol (75 mL) yielded off-white crystals of **4** (yield 95%). $\Lambda_M = 50\ \Omega^{-1}\ cm^2\ mol^{-1}$. Anal. Calcd for $C_{66}H_{65}BOsP_4$: C, 67.00; H, 5.54. Found: C, 66.92; H, 5.45.

The monodeuterated isotopomer $[(PP_3)Os(H)(\eta^2\text{-}HD)]^+$ (**4-$d_1$**) was prepared in situ by addition of a stoichiometric amount of $CF_3COOD$ to a solution of **3** in $CD_2Cl_2$ in a NMR tube. In the same manner, the di- and perdeuterated isotopomers (**4-$d_2$** and **4-$d_3$**) were prepared by reaction of **3-$d_2$** with stoichiometric amounts of $HOSO_2CF_3$ and $CF_3COOD$, respectively. Solid samples of **4-$d_3$** were obtained by precipitation with $C_2H_5OD$.

**Preparation of $[(PP_3)Os(H)(\eta^2\text{-}HAu(PPh_3)]PF_6$ (5).** A 0.09 g (0.18 mmol) sample of solid $[AuCl(PPh_3)]$ and $[NH_4]PF_6$ (0.10 g, 0.61 mmol) were added to a THF solution (25 mL) of 0.15 g (0.17 mmol) of **3**, under nitrogen atmosphere. The solution was stirred for 30 min. After reduction of the volume by distillation to ca. 10 mL, addition of ethanol (20 mL) led to the precipitation of cream colored crystals of **5** in a 80% yield, which were recrystallized from THF/$C_2H_5OH$ solutions. $\Lambda_M = 84\ \Omega^{-1}\ cm^2\ mol^{-1}$. Anal. Calcd for $C_{60}H_{59}AuF_6OsP_6$: C, 49.12; H, 4.05. Found: C, 48.94; H, 4.06.

**Preparation of $[(PP_3)Os(H)(N_2)]BPh_4$ (6).** Neat $CH_3OSO_2CF_3$ (0.032 mL, 0.28 mmol) was syringed into a THF suspension (15 mL) of **3** (0.23 g, 0.25 mmol) under an atmosphere of dry nitrogen. Upon addition of $NaBPh_4$ (0.20 g, 0.59 mmol) and ethanol (20 mL), lemon yellow crystals of **6** were obtained (yield 85%). $\Lambda_M = 48\ \Omega^{-1}\ cm^2\ mol^{-1}$. Anal. Calcd for $C_{66}H_{63}BN_2OsP_4$: C, 65.56; H, 5.25; N, 2.32. Found: C, 65.44; H, 5.38; N, 2.22.

**Preparation of $[(PP_3)Os(H)(CO)]BPh_4$ (7b). Method A.** Carbon monoxide was bubbled into a solution of **4** (0.10 g, 0.09 mmol) in refluxing THF (35 mL). On addition of ethanol (20 mL) and subsequent concentration under a stream of nitrogen, white crystals of **7b** precipitated (yield 80%).

**Method B.** Product **7b** can be obtained in ca. 95% yield by bubbling CO into a THF (25 mL) solution of **6** (0.20 g, 0.16 mmol) for 5 min at room temperature, followed by workup as described above. $\Lambda_M = 46\ \Omega^{-1}\ cm^2\ mol^{-1}$. Anal. Calcd for $C_{67}H_{63}BOOsP_4$: C, 66.56; H, 5.25. Found: C, 66.61; H, 5.15.

**Preparation of $[(PP_3)Os(H)\{\eta^1\text{-}CO(CH_3)_2\}]BPh_4$ (7d).** A $CH_3COCH_3$ solution (25 mL) of **6** (0.20 g, 0.17 mmol) was stirred during 30 min under an argon atmosphere. The mixture was then evaporated by distillation at reduced pressure (150 Torr) to give pale-yellow crystals of **7d** in a quantitative yield. $\Lambda_M = 51\ \Omega^{-1}\ cm^2\ mol^{-1}$. Anal. Calcd for $C_{69}H_{69}BOOsP_4$: C, 66.88; H, 5.61. Found: C, 66.76; H, 5.54.

**Reaction of 4 with Bases. (A) With K$^t$BuO.** Solid K$^t$BuO (0.09 g, 0.80 mmol) was added to a THF solution (20 mL) of **4** (0.20 g, 0.17 mmol) under a nitrogen atmosphere. The mixture was heated to reflux temperature during 15 min. On addition of ethanol, pale yellow crystals of **3** precipitated in ca. 95% yield.

**(B) With NaOEt.** Addition of a 3-fold excess of NaOEt, prepared in situ by dissolving the appropriate amount of sodium in absolute ethanol, to a THF solution of **4** prepared as above afforded pale yellow microcrystals of **3** in almost quantitative yield.

**(C) With $NEt_3$.** No reaction was observed between **4** and $NEt_3$ under analogous condition.

**Isotope Exchange Reactions. (A) With $D_2O$ and $CD_3OD$.** A weighted amount of **4** was dissolved in $CD_2Cl_2$ in an NMR tube. To the resulting solution, an excess (20 times) of either $D_2O$ or $CD_3OD$ was added via syringe at −78 °C. Variable-temperature NMR spectra ($^1H$, $^{31}P$) were recorded immediately after sealing the tube.

**(B) With $CD_3COCD_3$.** A weighted amount of **4** was dissolved in $CD_3COCD_3$ at −78 °C in an NMR tube, which was sealed. The H/D exchange reaction was then monitored by variable-temperature NMR spectroscopy.

**Table V.** Crystallographic Data for $[(PP_3)Os(H)(\eta^2\text{-}H_2)]BPh_4\cdot 0.5(CH_3)_2CO$

| | | | |
|---|---|---|---|
| chem formula | $C_{68}H_{69}B_1P_4Os_1O_{0.5}$ | $V$, Å$^3$ | 3016.23 |
| fw | 1212.20 | $Z$ | 2 |
| space group | $P\bar{1}$ (No. 2) | $\rho_{calc}$, g cm$^{-3}$ | 1.33 |
| $a$, Å | 16.841(4) | $\mu$(Cu K$\alpha$), cm$^{-1}$ | 52.94 |
| $b$, Å | 15.135(2) | $\lambda$,[a] Å | 1.5418 |
| $c$, Å | 12.450(3) | $T$, °C | 21 |
| $\alpha$, deg | 91.53(2) | $R$[b] | 0.047 |
| $\beta$, deg | 96.07(2) | $R_w$[c] | 0.052 |
| $\gamma$ deg | 106.75(2) | | |

[a] Graphite-monochromated Cu K$\alpha$. [b] $R = \sum||F_o| - |F_c||/\sum|F_o|$. [c] $R_w = [\sum(|F_o| - |F_c|)^2/\sum_w(F_o)^2]^{1/2}$.

**X-ray Diffraction Study.** Crystal data are summarized in Table V. A Philips PW1100 diffractometer with Cu K$\alpha$ graphite-monochromated radiation was used for the experimental work. A set of 25 carefully centered reflections was used for the centering procedure of the crystal. As a general procedure, three standard reflections were collected every 2 h (no significant decay of the intensities was observed). The data were corrected for Lorentz and polarization effects. Empirical correction for the absorption effect was performed at an advanced state of the structure refinement by using the program DIFABS.[36] Atomic scattering factors were those tabulated by Cromer and Waber[37] with anomalous dispersion corrections taken from ref 38. The computational work was performed on a Digital DEC 5000/200 computer by using the SHELX-76 system.[39] The final $R$ factors and the experimental and crystallographic data are reported in Table V.

The structure was solved by heavy-atom and Fourier techniques and refined by full-matrix least-squares methods. Anisotropic thermal parameters were used only for Os, P, B, and C atoms of the ligand. At an advanced stage of refinement two intensities of 0.6 e/Å$^3$ at the two cis positions of the octahedron around the osmium atom were considered potential H atoms. Although other spectroscopic evidence suggests the existence of the $H_2$ molecule at the position trans to the unique P atom of the ligand $PP_3$, the two H components could not be resolved. However, the refinement of the $H_2$ grouping as a single hydride ligand was relatively successful. In fact, the observed behavior was very similar to that pertaining to the classical hydride ligand undoubtely present in the cis position. All the phenyl rings were treated as rigid bodies with $D_{6h}$ symmetry (C–C = 1.39 Å), and the hydrogen atoms were introduced at calculated positions (C–H = 1.08 Å). The difference map also revealed the presence of a molecule of acetone solvent which was attributed a population factor of 0.5. The final difference map was featureless.

**Acknowledgment.** Thanks are due to the "Progetti Finalizzati Chimica Fine-II", CNR, Rome, Italy. A.P. thanks the DGICYT of Ministerio de Educación y Ciencia, Madrid, Spain, and the CIRIT of Generalitat de Catalunya, Barcelona, Spain, for a grant. The work of K.L. c/o ISSECC has been supported by a grant of the Commission of the European Communities.

**Supplementary Material Available:** Table S1, providing hydrogen atom locations for **4**, and Table S2, containing a complete set of crystallographic data for **4** (3 pages). Ordering information is given on any current masthead page.

(36) Walker, N.; Stuart, D. *Acta Crystallogr.* **1965**, *31*, 104.
(37) Cromer, D.; Waber, J. *Acta Crystallogr.* **1983**, *39A*, 158.
(38) *International Tables for X-ray Crystallography*; Kynoch: Birmingham, U.K., 1974; Vol. 4.
(39) Sheldrick, G. M. *SHELX76 Program for Crystal Structure Determinations*, University of Cambridge: Cambridge, U.K., 1976.